US.7
N56r3
V.27 no.5-6

SOCIOLOGY & ECONOMICS
DETROIT PUBLIC LIBRARY

SE

NAVAL RESEARCH REVIEWS

May-June 1974

SPECIAL ISSUE Naval Electronics Laboratory Center

Detroit Public Library
R 7 1975
Depository Document

PROFILES IN SCIENCE

Dr. Juergen H. Richter

Dr. Juergen H. Richter, an electronic engineer with a doctorate from Technical University, Munich, Germany, is responsible for tropospheric propagation research at the Naval Electronics Laboratory Center. With support from the Naval Electronic Systems Command and ONR, Dr. Richter developed a special microwave radar capable of observing atmospheric layers with a range resolution of one meter. This sensitive radar detects moisture and temperature structures in the clear atmosphere not previously observed.

Among his published papers is one on the application of conformal mapping to guided propagation around a curved earth. This paper provided for the first time a basis for rigorous analysis of the degree of approximation involved in using a modified refractive index for analyzing curved waveguides.

Dr. Richter recently has conducted an investigation of microwave ducting phenomena that occur close to the ocean surface. Using extensive measurements from the Pacific, Caribbean, and Mediterranean, techniques and procedures have been developed that permit the Navy to assess quantitatively the effects of the low-level oceanic duct.

Dr. Richter is a member of Commission Two of the International Scientific Radio Union. He received NELC's annual honorary award for scientific achievement in 1970.

Preface

Dr. C. E. Bergman, Technical Director
Naval Electronics Laboratory Center

As the principal Navy RDT&E Center for electronics technology and command control and communications concepts and systems, we at the Naval Electronics Laboratory Center believe our business is to help bring into being those electronic systems, equipments, and technologies most needed by the Navy and Marine Corps.

The improved capability needed to cope with new threats and missions as well as laboratory roles in providing such improvements has always been recognized. It is now becoming increasingly clear, however, that the systems and equipments of the future must also have low life-cycle-costs and reduced manning requirements, be highly reliable, and make more efficient use of available platform space and energy resources. Manpower and dollars, along with energy and space limitations, are fast becoming dominant factors in military procurement decisions. We therefore believe strongly that our work should be directed toward achieving these ends as well as improvements in performance.

Over the past few years we have thus taken decisive action to develop a second major thrust in our technical program to achieve these dual ends of performance and efficiency. This has been to develop a lead capability in applying the rapidly advancing technology of solid state electronics to achieve significant gains in equipment reliability, and reductions in equipment size, weight, and cost, and in energy and manpower requirements. The articles on the Quick and easy Design (QED) modules and the Modularized Digital Controller for Analog Power Drives are examples of this direction of effort.

We continue, of course, to put major emphasis on fulfilling the more traditional role of Navy laboratories in providing the technological base and the prototype systems development needed for future naval operations. Several articles in this issue provide examples of this type of work.

The entire Navy laboratory community has always played an important role in formulating RDT&E program plans by providing advanced system concepts and by cooperative planning with program managers and administrators in Washington. Although not treated specifically in any articles here, we believe our influence in this regard has been strengthened further through the recent formation of a group to provide systems engineering studies related to overall naval communications and command systems.

The articles in this issue of Naval Research Reviews can, of course, only touch upon a small sample of our total program. We are indeed grateful to the editorial staff of the Reviews for providing us this forum, and we hope the articles will illustrate in some measure the broad scope of our RDT&E activity and the wide variety of its important naval applications.

Radio Propagation in a Marine Environment

J. H. Richter and H. V. Hitney
Propagation Technology Division
Naval Electronics Laboratory Center

Microwave radio propagation in a marine environment frequently exhibits unexpected behavior. These propagation anomalies are usually caused by nonstandard distributions of the refractive index profile. In the case of shipboard radars, targets can sometimes be seen at distances far beyond the normal radar detection range. Famous examples of greatly extended ranges include the sighting of the Arabian coast with vhf radars in India, which is 1500 miles distant, and the reception of vhf signals from Hawaii in San Diego, California, which is 2500 miles distant.

The same atmospheric conditions that are responsible for range extensions may also cause electromagnetic (EM) energy to be channelled or "ducted" away from regions that would otherwise be illuminated. In the case of radar, a so-called "radar hole" may be created. EM ducting phenomena are particularly dramatic and frequent in a marine environment. The most unusual propagation anomalies result when dry, warm air masses advect over cold, moist marine air, thereby creating layers of different refractive index. A very persistent ducting phenomenon is a low-level duct directly above the water, which is caused by evaporation from the surface.

Since different analytical and experimental methods are required in investigating propagation anomalies caused by the oceanic evaporation duct and by elevated refractive layers, it is convenient to distinguish between the two phenomena. Thus, the following sections describe the Naval Electronics Laboratory Center's efforts to (1) calculate, measure, and predict propagation conditions in the oceanic evaporation duct, and (2) develop and apply remote sensing techniques for assessing the effect of elevated refractive structures on radar, communication, and electronic warfare.

Oceanic Evaporation Duct Propagation Phenomena

The vertical decrease of relative humidity from 100% at the air-sea boundary to some lower value above that point results in a rapid vertical decrease of the refractive index. Electromagnetic waves

travelling close to the water surface may be significantly influenced by this refractive index distribution. In extreme cases, they may be very efficiently ducted.

Figure 1 shows two vertical distributions of the modified refractivity profile. Modified refractivity is defined as

$$M = (n - 1) \times 10^6 + \frac{h}{a} \times 10^6$$

where n is the refractive index, h is the height above the surface, and a is the earth's radius. The dashed line would occur during conditions of no evaporation ducting, while the solid line would be representative of good ducting conditions.

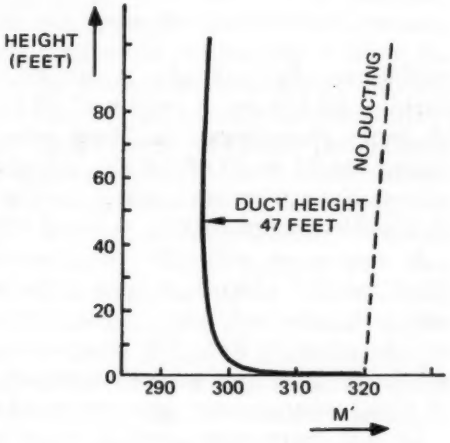

Figure 1 – Modified refractivity profile M for no ducting (dashed curve) and for a 47-foot duct height (solid curve).

Figure 2 shows the vertical distribution of path loss for the two refractivity distributions of Figure 1, assuming a 21-mile, 9.6-GHz, over-water propagation path with one terminal located 16 feet above the water. Path loss is the ratio in decibels of transmitted to received power, assuming isotropic antennas. In this case, the dashed curve indicates a decrease of path loss (or an increase of signal) with height. The solid curve, which corresponds to the solid modified refractivity curve in Figure 1, shows a minimum in path loss (or a maximum in received signal) at a height of about 15 feet. The signal enhancement shown at this height emphasizes the importance of the oceanic evaporation duct to naval operations.

The presentation in Figure 2 may also be used to determine which antenna heights would provide optimum utilization of ducting

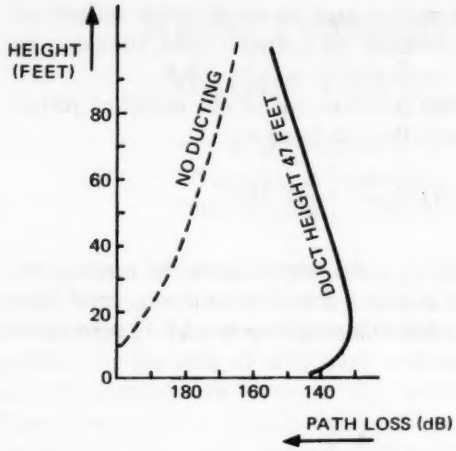

Figure 2 – Path loss profiles for a 9.6 GHz, 21-mile path, with a terminal height of 16 feet. The dashed curve is for no ducting and the solid curve is for a 47-foot duct height.

conditions. For example, it can be seen that an antenna at a height of 64 feet would receive 11 dB less signal than an antenna at 15 feet. Nonetheless, the signal enhancement from evaporation ducting would be 30 dB for the high antenna. The fact that signal enhancements from evaporation ducting are usually encountered at all possible antenna heights on board ship is frequently overlooked.

A convenient parameter for describing ducting conditions is "duct height," which is defined as the height at which the M-curve attains its minimum value. Thus, the solid curve in Figure 1 has a duct height of 47 feet. This parameter should not be misinterpreted as a height limit for signal enhancements. As shown in Figure 2, 30 dB signal enhancements are experienced well above the duct height.

So that evaporation ducting would be properly recognized and utilized for Navy operational problems, NELC conducted an extensive analytical and experimental program. The four objectives of this program were as follows:

- Develop methods to calculate radio propagation under evaporation ducting conditions,
- Determine the meteorological measurements necessary to describe ducting,
- Investigate the feasibility of using long-term meteorological data to estimate ducting conditions for any oceanic area, and
- Investigate the effectiveness of ducting on various antenna heights.

The first objective was met by developing a computer program for calculating propagation parameters in a leaky wave guide, such as the evaporation duct. Propagation losses from atmospheric absorption

and scatter from a rough sea surface are incorporated in this computer program. Although not all of the physical processes in the marine boundary layer are fully understood, the refractivity profile necessary to describe adequately propagation conditions can be determined from simple meteorological measurements that are easily obtained under operational conditions. The necessary parameters are water temperature measured at the surface and air temperature, relative humidity and wind velocity all measured at some predetermined height (e.g., bridge height). It was found that long-term meteorological observations of these parameters provide a good basis for estimating ducting conditions for any oceanic area for which data are available.

To meet the final objective, NELC conducted an extensive experimental program with measurements in the Southern California off-shore area, in the Key West area, and in the Eastern Mediterranean. The measurements made were designed to provide data to check the mathematical models, to compare with meteorological statistics, and to determine which antenna heights would provide optimum utilization of the evaporation duct. To determine the relative performance of high- and low-sited antennas, measurements were made between terminals on the islands of Mykonos and Naxos in the Aegean Sea during two-week periods in each of the four seasons. Various frequencies were transmitted from the Naxos terminal and were received on vertically-spaced antennas installed at the Mykonos terminal. The path length was 21 miles and the terminal heights were 16 and 64 feet above sea level. Figure 3 is an example of measured data at 9.6 GHz presented in terms of actual radar performance. It translates measured propagation data into detection ranges for a radar having a 200-nautical-mile free-space detection range. Under no ducting conditions, the detection range would have been 16 nautical miles. Figure 3 illustrates the fact that surface-to-surface detection ranges are almost always significantly enhanced by evaporation ducting.

Optimum antenna height can be determined only if the radar parameters and the area and season under consideration are known. If the geographical region and season cannot be specified, the best antenna location for longest detection ranges would be the highest possible site aboard ship.

Remote Sensing of Refractive Layers

Elevated refractive layers, unlike evaporation ducts that are important only for propagation close to the ocean surface; can influence

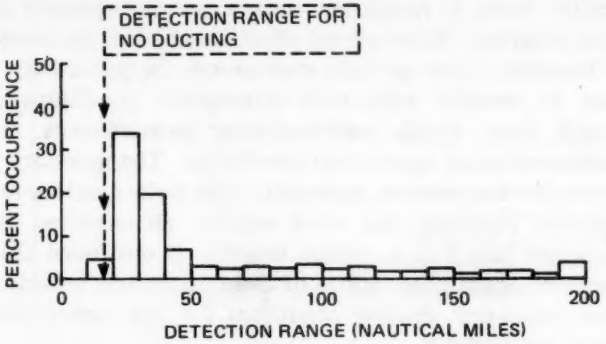

Figure 3 – Distribution of detection ranges for a 9.6 GHz radar with a 200-nautical-mile free-space detection range based on measurements made in the Eastern Mediterranean.

detection ranges for any target or receiver altitude. These layers can be found up to heights of at least 10,000 feet. Because of the height variability, it is difficult to determine properties of elevated layers from direct sensing measurements. A further complication arises when elevated layers are horizontally inhomogeneous in a manner that affects propagation. A tilt in a refractive layer caused by atmospheric waves may result in propagation anomalies.

For the above reasons, NELC's investigation in this area has concentrated on improving refractive index measurement and forecasting techniques. NELC researchers realized that only remote sensing techniques would be capable of providing answers to some of the fundamental questions, such as temporal and spatial refractive microstructure. Therefore, a special active remote sensor was developed–a frequency modulated, continuous wave (FM-cw) radar. The remarkable success of this device is due to the combination of three features–high-range resolution (1 meter), high sensitivity, and close minimum range without clutter. Two such radar units are presently in use at NELC. One has fixed, vertically pointing antennas and the other is a mobile unit with scanning capability (1, 2).

The radar sounder observation shown in Figure 4 demonstrates the sounder's ability to sense microstructural details in the atmosphere. In this presentation, the radar sounder was pointed vertically, thereby creating a time versus height display. Several distinct strata of various vertical and temporal behavior can be seen in Figure 4. The refractive index profile obtained from a radiosonde sounding at 1235 PST is superimposed over these strata. The agreement of backscatter zones and refractive index gradients is remarkable.

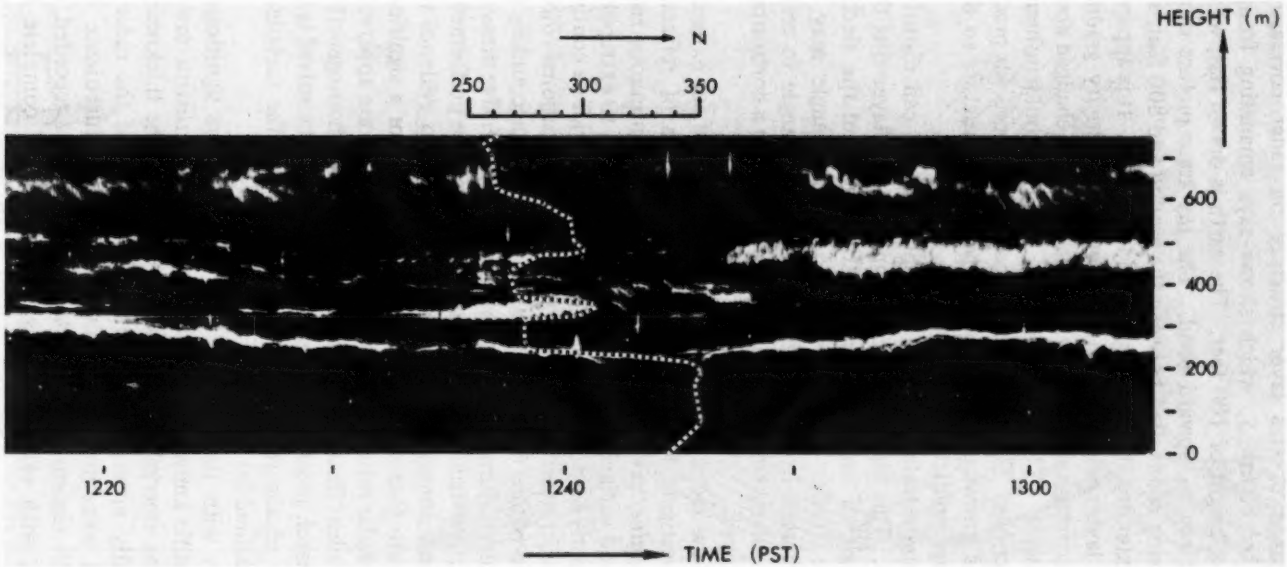

Figure 4 – Refractive layers in the atmosphere as observed with NELC's FM-cw radar sounder. The dashed curve is the refractivity $N = (n - 1)\,10^6$ (where n = refractive index) measured with a sounding balloon.

The significance of this layer structure on radar coverage is demonstrated by Figure 5, which shows rays emanating from a transmitter at a height of 100 feet. The earth is drawn flat, which gives a straight ray an upward bend. The ray trace picture shows radio energy being channelled between the ground and 800 feet, and indicates the extended detection ranges in this region. It is apparent that only the layer belonging to the steepest refractivity gradient influences the coverage significantly. This layer height changed about 80 meters between 1220 and 1240 PST, and this could influence coverage predictions. This example emphasizes the need for precise and continuous knowledge of the refractive index structure so that accurate coverage predictions can be made.

Figure 6 demonstrates how an atmospheric wave can disturb a layer structure. This kind of wave motion results in layer tilts that change the angle of incidence between the layer and the electromagnetic wave front. At some point, the new angle may be sufficiently different from the original undisturbed angle to create propagation problems that would not be expected from a horizontally homogeneous layer.

NELC's FM-cw radar sounders have been operated for extended periods to investigate the structures and scale sizes of refractive layers. Procedures have been developed to use continuous radar sounder data and surface meteorological observations to extrapolate temporally directly-sensed profiles. This method provides a continuous update of refractive profiles using only occasional direct soundings. The nature of the backscatter mechanism accounting for the radar sounder returns has been investigated. Extensive measurements of refractive structures using both sounders were performed at both normal and nonnormal angles of incidence. No evidence was found to indicate that specular reflections account for a significant portion of the radar returns. Rather, the radar echoes are apparently caused by turbulent distribution of refractive index inhomogeneities. The major research problem in this area remaining to be solved is the reconstruction of the refractive index profile from the turbulence parameters measured by the radar.

Observations with the FM-cw radar sounders have significantly increased scientific knowledge of the tropospheric microstructure. A new picture has emerged of thin scattering layers, the thickness of which frequently approaches the range resolution of the radar (1 meter). What sometimes appeared to be random turbulence was discovered to be organized substructure. The sounder recorded, for the first time, with very high range resolution the complete life cycle of shear-induced stabilities, which is an important dynamic

550-896 O - 74 -- 2

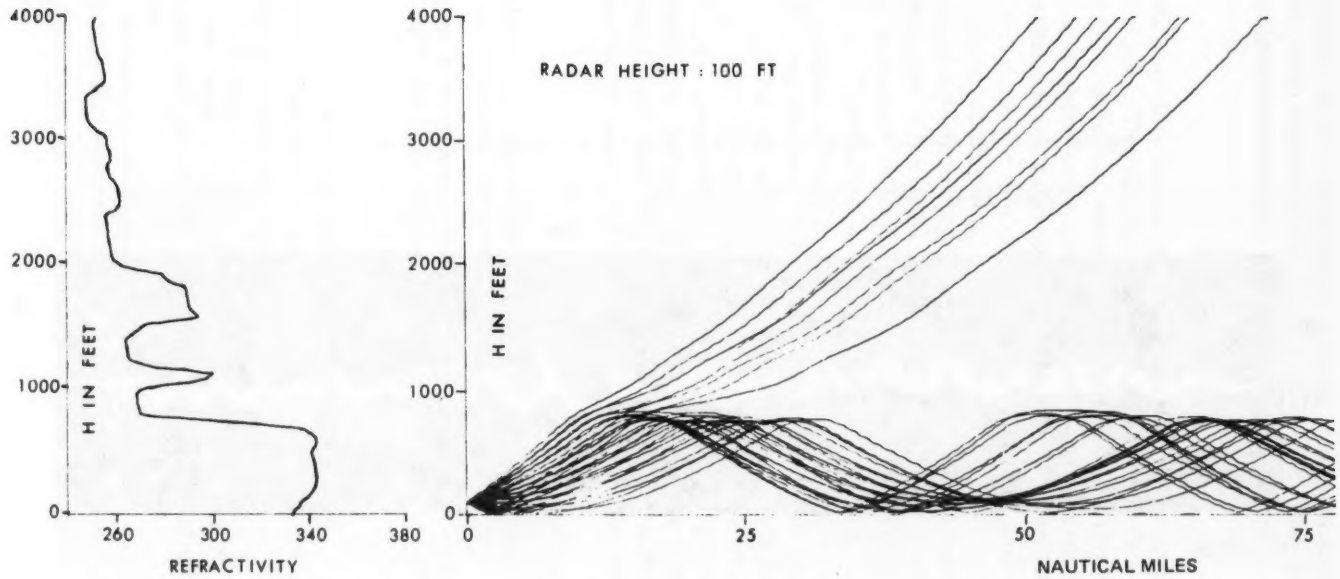

Figure 5 – Ray trace for the refractive conditions of Figure 4. Rays emanate from a radar at a height of 100 feet.

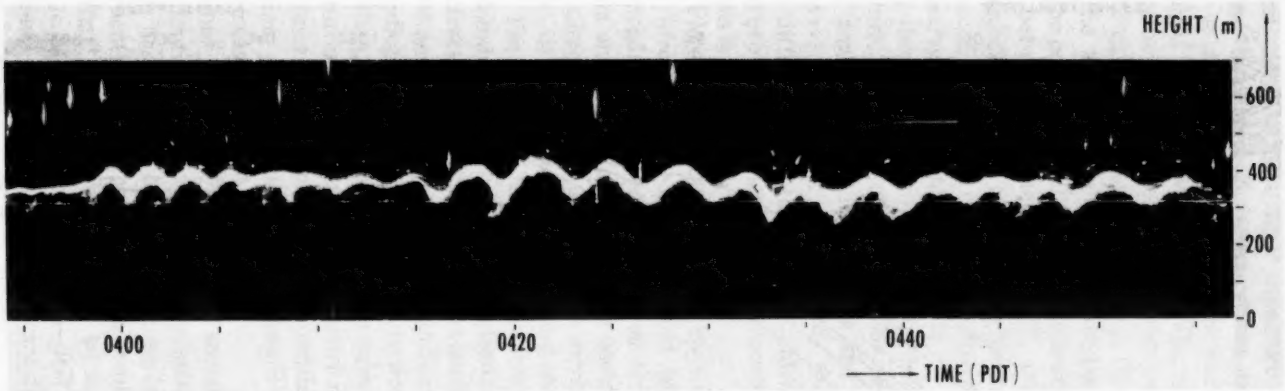

Figure 6 – FM-cw radar sounder observation of a refractive layer perturbed by wave motion.

phenomenon in the atmosphere. Radar reflectivities previously measured with radars having much coarser resolution were found to be underestimated by one to two orders of magnitude.

Conclusions

A low level duct caused by evaporation is found most of the time over all oceans. This duct has a significant effect on surface-to-surface detection ranges of microwave radars. An extensive investigation of this ducting phenomenon has shown that propagation conditions can be calculated based on simple in-situ measurements and that probability of occurrence of ducting conditions can be estimated from meteorological statistics.

A unique active remote sensing system, the FM-cw radar sounder, was developed in an effort to improve the ability to recognize and predict anomalous radio propagation caused by elevated refractive structures. Observations with this sounding technique have significantly changed scientific understanding of tropospheric microstructure. It is apparent now that remote sensing techniques are measurement tools that are needed for solution of anomalous propagation problems, even though questions remain to be answered before full operational implementation will be possible. It is expected that the combination of different remote sensing techniques, such as radar sounders, acoustic sounders, laser sounders, and radiometric methods, will enhance the Navy's capability to sense its operating environment.

References

1. Richter, J. H., "High-resolution Tropospheric Radar Sounding," *Radio Sci.*, v. 12, p. 1261-1268, December 1969

2. Richter, J. H., Jensen, D. R., and Phares, M. L., "Scanning FM-cw Radar Sounder," *Rev. Sci. Inst.*, v. 43 (11), p. 1623-1625, November 1972

Bit Error Rate (BER) Monitoring Unit

NELC has developed a link monitoring unit that provides a means for long-term unattended communications link performance monitoring. The unit consists of a bit error rate (BER) monitor and a high-speed digital printer. It outputs error count in real time on a light-emitting-diode (LED) display and permanently on paper tape. Thus, it is suitable for both attended and unattended operation.

The BER monitor contains a transmit code generator and a receive monitor that automatically locks onto a selected received data stream and compares it to

(Continued on page 24)

RF Susceptibility of Microelectronic Components

A. R. Hart, D. W. McQuitty, and N. K. Wagner
Microelectronics Division
Naval Electronics Laboratory Center

Field experience and laboratory investigations indicate that a significant percentage of premature or unexpected failures of electronic parts and equipment during Fleet operations is related to high-intensity radiated rf energy, such as that caused by radars found on all Navy ships. Degradations or failures have been reported in aircraft during carrier landings and in electronic components during replenishment and repair operations in rf environments. Three approaches to solving this problem would be to investigate new operational procedures, change equipment and circuit designs, and/or reduce the rf susceptibility of electronic devices used in Navy equipments. The Naval Electronics Laboratory Center has investigated the extent of damage to microelectronic components when exposed to high-intensity electromagnetic radiation, specifically, how microelectronic device susceptibility is related to rf-induced damage. The program, sponsored by NAVELEX, was performed in cooperation with the Naval Weapons Laboratory (NWL), Dahlgren, Virginia. Its dual objective was to (1) determine the relationship between semiconductor processing defects and injected rf failures in microelectronic devices, and (2) investigate the feasibility of using a process screen to reduce rf susceptibility of electronic components in Navy equipments.

In an initial study of device susceptibility conducted in 1972, an investigation was made of failures in semiconductor repair parts caused by direct irradiation by radar sources. It was found that electronic repair parts being transferred from ship to ship during underway replenishment operations were subjected to high-intensity rf energy, even though they were still encased in their normal paper or plastic packages. This rf radiation caused failures and degradations in many types of semiconductor devices ranging from diodes to integrated circuits. Further testing showed that the number of failures related to rf irradiation was not reduced significantly when aluminum-lined packages were used, and that package quality (such as scratches or breaks in the material) affected the protection provided by the package in rf environments (1). As a result, the Navy has recommended

that microelectronic devices be packaged in materials that prevent damage in rf environments during replenishment operations.

During this initial NELC study, unexplained variations in device failure levels were found that were tentatively attributed to factors inherent within the device, such as defects in the silicon chip or contamination introduced during processing. Also, many types of irregularities were found in the failed devices. These findings led to the program described in this paper.

Transistor Rf Susceptibility

An investigation was made to determine the relationship between transistor rf susceptibility and (1) process control defects, (2) transistor physical defects, and (3) electrical characteristics. These transistor studies would also apply to such complex microelectronic structures as integrated circuits and could lead to improved manufacturer process screens and controls.

Results of the investigation (2) indicated that the rf susceptibility of transistors may be reduced by screening four defects during the processing phase of transistor construction. These defects, which significantly affected the rf susceptibility of transistors, were:

- Pinholes, pits, or voids in the oxide or diffusion regions,
- Flakes of metallization (including extrusions caused by a scratch or by overbonding),
- Undercut oxide or diffusion layers (including defects in oxide mask, and
- Voids in metallization or metallization width reduced.

Bipolar transistors chosen for the investigation were representative of those used in Navy electronic equipments for non-rf environment applications. Ten categories–five types of transistors from each of two manufacturers–were selected for testing. NELC was responsible for transistor preparation, physical and electrical characterization, computer analysis of pre- and post-rf results, and failure analysis of the damaged devices. NWL subjected the test transistors to the rf source.

The pre-rf characterization consisted of low- and high-power optical inspections, scanning electron microscopy (SEM) analysis, and extensive electrical tests for each of 842 transistors. The post-rf characterization consisted of the same procedures to identify the failure modes of all transistors, plus metallurgical etching and cross-sectioning to investigate the physics of failure. Computer analysis of pre-rf physical and electrical characterizations and post-rf failure

data resulted in significant correlations between the four defects listed above and the rf susceptibility of transistors.

Correlations were also found between device design (e.g., geometry considerations), failure level, and failure mode. For example, devices using a "C"-shaped geometry emitter pattern showed "surface deformation of the aluminum metallization" as their major failure mode. In this mode, as shown in Figure 1, the aluminum and silicon melt due to the extreme heating from the injected power and fuze together to form a physically deformed area on the metallization pattern. The experiment showed that more than 50 percent of the transistors in seven of the ten categories had this type of failure mode. On the other hand, devices using the interdigitated geometric pattern usually showed "lateral tunneling between the emitter and base metallization patterns" as the major failure mode. This mode can be described as a melted silicon filament connecting the emitter and base metallization patterns. Figure 2 shows the surface and corresponding subsurface junction image of this type of failure mode. Since geometric design of the silicon chip does affect the rf

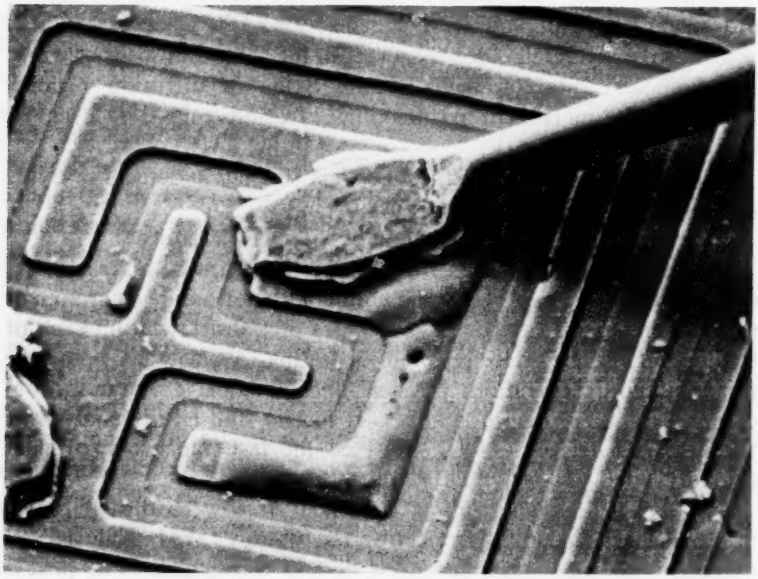

Figure 1 – Scanning electron microscopic view of "surface deformation of metallization" failure mode. The lateral tunneling is a subsurface effect where silicon has been melted, creating a channel between the emitter and base metallization contacts. Aluminum is usually found in the channel.

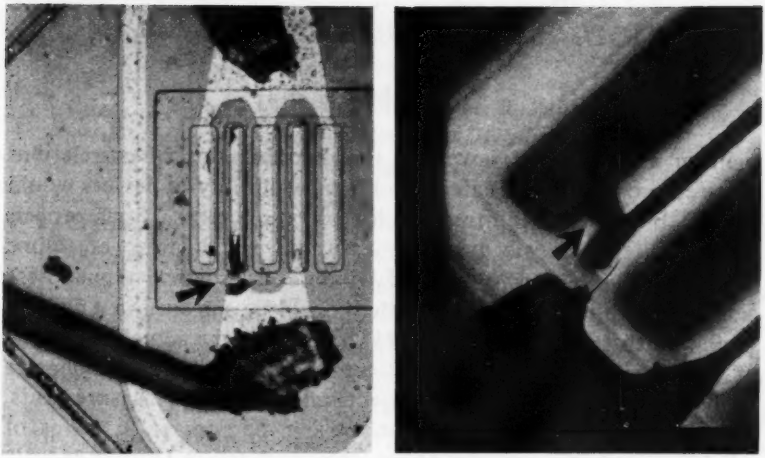

Figure 2 – The photomicrograph at left shows a transistor having the failure mode of "lateral tunneling" between the emitter and base contacts. The figure at right is a SEM photo of the same transistor showing the junctions within the silicon chip. The tunnel can be seen in both figures (arrows). A base metallization path has melted, causing a physical and electrical open to the base contact area.

susceptibility of the device, the circuit designer or systems engineer has the option of selecting components that are less susceptible to rf damage by geometry considerations. This is one approach that, when combined with good system engineering, will increase the life expectancy of electronic equipment used in high-intensity rf environments.

Impact of Device Rf Susceptibility on Fleet Effectiveness

The second area defined by the transistor investigations involved the present definition of rf susceptibility problems in the Navy. Energy from spurious electromagnetic fields can be injected into equipment circuitry by the coupling of these fields with system interconnections. The investigations showed that such injected energy may physically damage the aluminum metallization without causing the device to fail electrically. Thus, even though the electrical operation of electronic equipment subjected to coupled-in microwave energy is unaffected at the time of exposure, that equipment's reliability and life expectancy would be reduced by the metallization

damage, and its effectiveness under emergency conditions would be questionable.

Conclusion

From a preventive viewpoint, the determination of correlations between process-related defects and rf susceptibility of devices would provide background information for process screens. Such process screens are theoretically possible because several defects were found to be statistically correlated to rf failure of transistors. Since these defects are optically observable, they could be screened in a manner similar to that outlined in MIL-STD-883 during the actual processing of the transistors. It was also determined that rf-induced damage cannot always be defined by electrical parameter measurements. Therefore, rf damage to Fleet electronic equipment in terms of reliability and life expectancy may be more severe than previously reported.

The investigations currently being conducted will further define the areas discussed above and determine:

- If protective measures exist as temporary solutions to the rf susceptibility problem,
- How ambient temperatures affect the rf susceptibility of devices, and
- Whether integrated circuits of the metal-oxide-semiconductor (MOS) type will be more or less susceptible to rf energy than the bipolar types. This is important since the microelectronics industry is making increased use of MOS-type devices to perform the functions previously performed by bipolar integrated circuits.

By applying the information generated in the rf susceptibility programs, it is expected that Navy electronic systems operated in typical Fleet environments will be more reliable and that maintenance time and costs will be reduced.

References

1. Naval Electronics Laboratory Center Document 204, *Rf Protection Provided by Packaging Materials*, by A. R. Hart and R. P. McCluskey, 27 September 1972

2. Naval Electronics Laboratory Center Report 1902, *Rf Failure Mechanisms Related to Microelectronics Process Control*, by A. R. Hart, N. K. Wagner, and D. W. McQuitty, 5 December 1973

Equatorial Scintillation

R. U. F. Hopkins and M. R. Paulson
Uhf Technology Division
Naval Electronics Laboratory Center

For many years, radio astromomers have observed that signals from radio stars received at a fixed ground station scintillate, or fluctuate in amplitude. At first they thought the fluctuating signal strength was caused by fluctuation in the power of the source (the radio stars). However, spaced receiver tests have shown that irregularities in the electron density of the ionosphere caused the signals to scintillate as the source moved or as the irregularities moved through the propagation path.

With the development of artificial satellites, many new radio sources became available for the study of the scintillation phenomenon. At the same time, it became very important to know what effect the ionospheric irregularities would have on transmissions to and from these satellites.

It is believed that the electron-density irregularities occur in the F region of the ionosphere. Kent and Koster (1) report measuring irregularities at heights from about 240 km up to about 400 km. The irregularities are elongated, with the longer axis parallel to the earth's magnetic field lines. Axial ratios greater than 60 to 1 have been measured.

The most frequent and intense scintillation activity occurs in the auroral regions and in a region along the magnetic equator at night. The sporadic activity along the equator tends to be greatest around the equinoxes, and is most intense during periods of high sunspot number.

Although it appears that the generation of electron-density irregularities that cause scintillation is dependent on solar activity, no direct cause-effect relationship has as yet been established. Several theories have been advanced to explain this generation, but none is considered completely satisfactory.

Since the refractive index of the ionosphere is a function of radio frequency, irregularities in the ionosphere will have progressively less effect as the transmission frequency is raised. However, the rate that the scintillation intensity decreases with increasing radio frequency is not known. Various researchers have estimated that it is inversely proportional to frequency; others, that it is inversely proportional to frequency squared; and one, that it is inversely

550-896 O - 74 -- 3

proportional to the square root of frequency. It appears that the frequency dependence is not constant and may vary with ionospheric conditions. In one instance, measurements of peak-to-peak scintillation were made that were greater than 6 dB at 6 GHZ.

Since the Navy plans to increase the use of satellites in communications and navigation, it is important to know how scintillation activity will affect such systems. While considerable research has already been done, most of it was conducted at frequencies below 100 MHz. Also, results of many of these studies were presented in terms of scintillation indices that are not very useful for engineering purposes. Consequently, the Naval Electronics Laboratory Center was requested to make some measurements in the equatorial region so that the problem in that area could be evaluated. This article discusses results of studies made during three trips to the Pacific equatorial region in 1970, 1971, and 1972.

Experimental Investigations

Figure 1 is a typical example of a recording of the equatorial scintillation phenomena made on Guam from 250 MHz TACSAT-1 signals. Attention is directed to (1) the rapid scintillation buildup at left, (2) the very rapid nature of the fading, and (3) the enhancement of signals that accompany deep fading. The latter point suggests that some form of multipath channel exists. Measurements obtained by the Instituto Geofisico del Peru using the ionospheric radar at Jicamarca, Peru confirm that the irregularities of electron density responsible for scintillation are widely distributed above the F layer, suggesting that multiple scattering may be the propagation mechanism in effect. Further theoretical and experimental research will be necessary before the nature of the interaction of electromagnetic waves with ionospheric irregularities can be stated with assurance.

The question of how the irregularities are formed in the first place is even more of an enigma. Solar energy inputs are certainly necessary. This is demonstrated in Figure 2, which compares scintillation activity to the monthly mean relative sun spot number occurring during the three NELC experiments. Although the scintillation activity appears to follow the monthly mean number rather well, comparison of the two on a daily basis indicated no correlation at all—regardless of positive or negative time delay offsets between the daily values.

Statistical analysis was performed on recordings of the type shown in Figure 1 to derive such information as cumulative amplitude

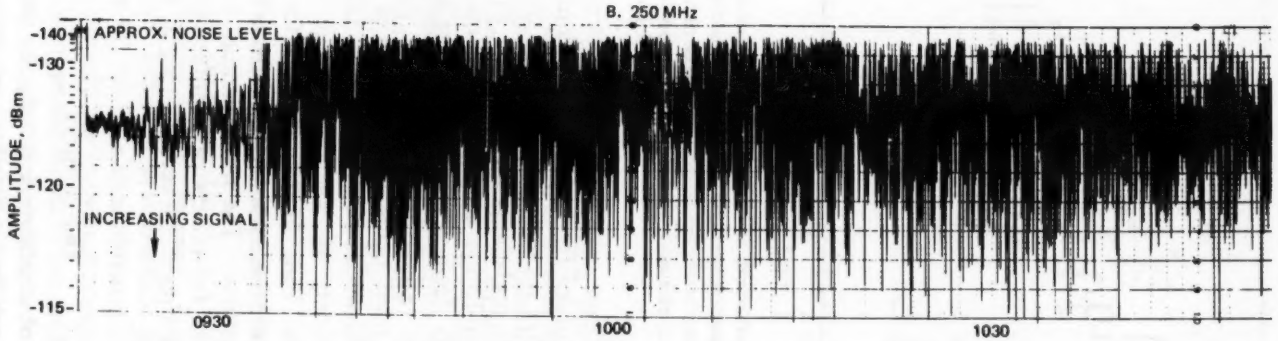

Figure 1 – Example of scintillation activity recorded on Guam from 250 MHz TACSAT I signals on 11 October 1972 GMT.

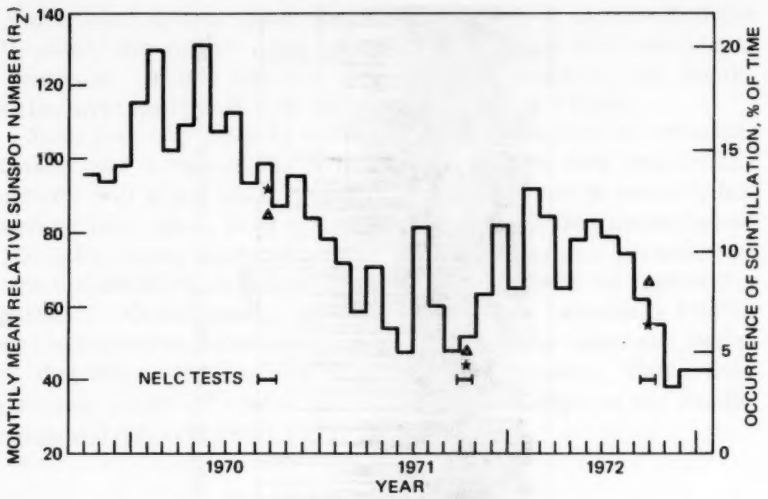

Figure 2 – During NELC's equatorial scintillation experiments in 1970, 1971 and 1972, scintillation activity was compared to the monthly mean relative sun spot number. In this figure, △ = the occurrence of scintillation and ★ = the average of the daily relative sun spot numbers for the periods of each of the NELC tests.

probability distributions, envelope power spectrum densities, and fade duration distributions for systems applications. Figure 3 shows the temporal variation of several levels taken from a number of cumulative amplitude probability distributions. From the figure, it is apparent that scintillation activity commences abruptly in the evening and gradually declines into the morning hours. Thus, it is evident that satellite systems operating in the military uhf band could be subject to many hours of degradation or complete disruption. Analysis of numerous power spectra of the signal envelope indicated that practically all components were below 1 Hz and usually below 1/2 Hz. Fade duration statistics for 6 dB and 12 dB below the mean signal level were developed from the data for use in error control applications. The results indicated that any system designed to overcome the effects of scintillation must be able to handle signal fadeouts up to 10 seconds long at 6 dB and up to 5 seconds long at 12 dB.

Dependencies

The dependence of scintillation activity on such parameters as latitude, elevation angle to the satellite, and carrier frequency was

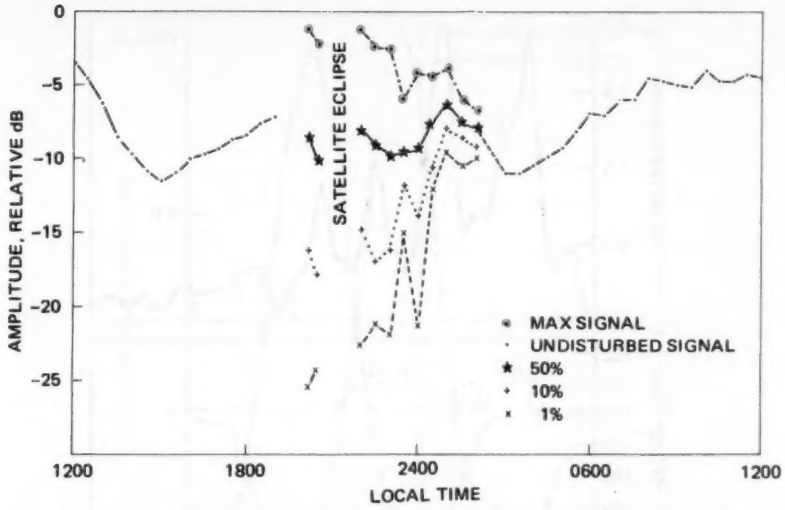

Figure 3 – In this experiment, four points from the cumulative amplitude probability distributions of TACSAT I uhf signals were plotted during periods of scintillation activity. The four points were maximum signal level, and 50%, 10%, and 1% probability. When no scintillation was occurring, the undisturbed signal level was recorded.

also investigated. Briefly, it was found that scintillation in the equatorial region occurs primarily in a band approximately 15° of latitude from the geomagnetic equator. Elevation angle dependence is slight. Simultaneous measurements of signals from TACSAT-I at 250 MHz and 2300 MHz indicated that scintillation intensity was 25 dB less at 2300 MHz, as measured between the cumulative amplitude probability distributions at 99% probability. *Thus, it is suggested that strong consideration be given to use of the higher frequencies for space services.*

Drift Velocity of the Ionospheric Irregularities

Measurements to determine the vector drift velocity of the ionospheric irregularities were made using a triangle arrangement of receivers placed on East-West and North-South baselines. Cross spectrum analysis of the data thus obtained yields the speed and direction of drift velocity for individual components of the fading spectrum. Figure 4 shows the results of one such measurement. The reason for using the complex analysis was to determine if the fading was due to one component of drift velocity or possibly more than

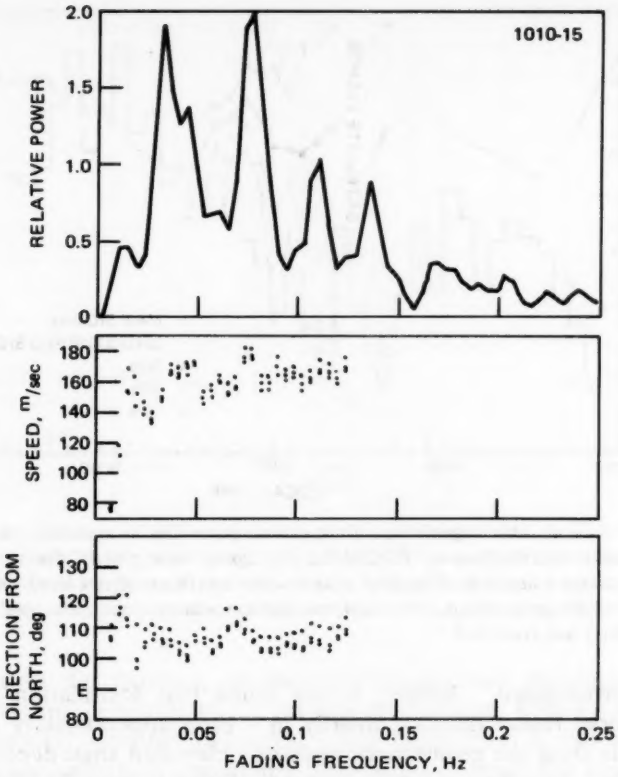

Figure 4 – By analyzing the drift velocity of ionospheric irregularities, it was possible to determine the speed and direction of drift veolcity for individual components of the fading spectrum. This data was recorded on Guam, 28 October 1971 GMT.

one component with different directions. It is evident from the results that all components of the fading spectrum had a common drift velocity.

Valuable information on the spatial diversity characteristics of scintillation fading was also obtained from the drift velocity experiment. Figure 5 shows the correlation between pairs of received signals as they are displaced in time. As expected, the N-S elongation of the irregularities combined with an eastward drift velocity results in high correlation at zero time delay while the E-W pair exhibits a high degree of decorrelation. The peak correlation of the E-W pair at 6 seconds delay provides the necessary information needed to compute drift velocity in that direction. This data provided

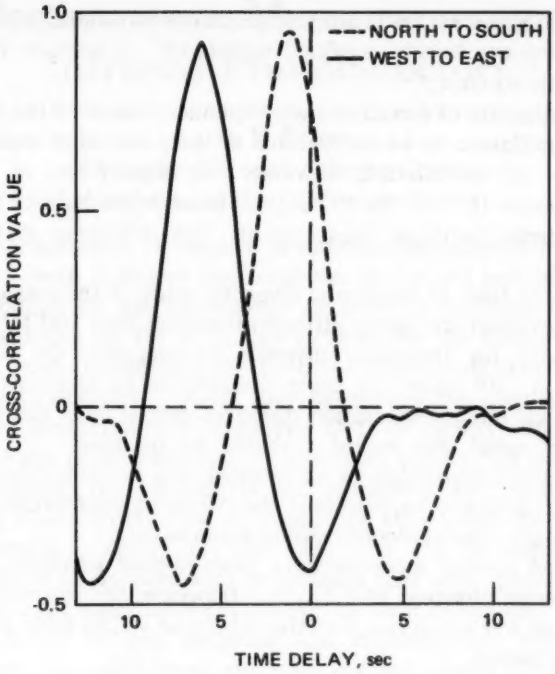

Figure 5 – Cross-correlation values were calculated for spaced-receiver triangle arrangement for records made on Guam from 1255 to 1300 GMT, 28 October 1971. West-East spacing was 1100 meters, and North-South spacing was 750 meters.

the basis for the design of a space diversity system to be used at Guam to minimize the effects of scintillation fading.

Conclusion

The results of NELC's equatorial scintillation investigations are detailed in reference 2 and summarized below.

- The uhf scintillation near 250 MHz was very intense (exceeding 25 dB peak-to-peak) and faded quite regularly into the system noise. This scintillation was predominantly a nighttime phenomenon, usually starting within an hour or two after ground sunset and often occurring until 1:00 or 2:00 a.m. (local time). On one or two occasions, scintillation occurred until 4:00 or 5:00 a.m.
- Samples of scintillation data for three successive years indicate that scintillation occurrence varies with solar activity.

- Investigation of the latitude dependence of scintillation showed that activity was largely confined within 15° of latitude from the geomagnetic equator.
- Investigation of elevation-angle dependence showed the intensity of the scintillation to be comparable at three elevation angles. The occurrence of scintillation, however, was slightly less at the 72° elevation angle than at the 30° angle. However, because of the short time converted in these measurements, this difference may not be significant.
- Limited tests of frequency diversity made in the region of 250 MHz suggest that frequency differences greater than 100 MHz would be necessary for frequency diversity to overcome the effects of scintillation. In order for space diversity to be effective in overcoming such effects, separation distances greater than the length of the largest naval ship would probably be required.
- Statistical evaluation of the scintillation records indicates that any system designed to overcome the effects of scintillation must be able to handle signal fadeouts several seconds long.
- During limited measurements, peak-to-peak scintillations of 2 to 5 dB were observed at 2.3 GHz. However, the intensity of this scintillation was much less than that observed at 250 MHz during the same time period.

References

1. Kent, G. S. and Koster, J. R., "Some Studies of Nighttime F-Layer Irregularities at the Equator Using Vhf Signals Radiating from Earth Satellites," *Annales de Geophysique*, v. 22, no. 3, p. 405-417, 1966

2. Naval Electronics Laboratory Center Technical Report 1875, *Effects of Equatorial Scintillation Fading on SATCOM Signals*, by M. R. Paulson and R. U. F. Hopkins, 8 May 1973

(Continued from page 11)

the transmitted reference code to determine the number of errors. It provides continuous service, even at high error rates. If the signal is lost, it is automatically reacquired without operator intervention.

Five monitoring units were fabricated by NELC for use during operational evaluation (OPEVAL) of the Satellite Fleet Broadcast Receiver (SSR-1). Four were used aboard ship and one was used for monitoring bounce back at the transmit station. During OPEVAL, the printout device of the unit provided time-of-day information, mode of operation (FM or PSK), sample size, and error count. These units were subsequently used in the WSC-3 radio set OPEVAL and are now being operated in connection with various NELC projects.

Development of the BER monitoring unit was sponsored by NAVELEX.

Performance Measurements of Infrared Photodetectors

R. F. Potter
Electronic Materials Sciences Division
Naval Electronics Laboratory Center

The developments in modern semiconductor material technology have been both intensive and extensive in nature, and have had a special impact on the technology of infrared radiation detection. Certain agencies of the U. S. Navy, including the Office of Naval Research, early recognized the need for conducting research in IR detection technology. Thus, they sponsored the concept of and tasked the formation of a Tri-Service DoD IR facility, which is now located at the Naval Electronics Laboratory Center, for the purpose of establishing the parameters for describing and reporting the operating characteristics of all classes of IR photodetectors. The most important aspect of this task was the development and establishment of measurement procedures that were appropriate and required for the quantitative evaluation of these detectors.

As a result of this program and collaboration with the IR community, the established methods and procedures for measuring and describing IR transducers are far and away superior to those available for other transducers. Measurements of characteristics made at one facility can not only be duplicated at another with relatively little ambiguity in reporting and interpretation procedures, but can also be reasonably extrapolated and interpolated to apply to operational conditions not necessarily used in the measurement laboratory.

Although the conditions under which a detector may be measured and used are almost infinite in number, the number of parameters must be limited in order to establish a standard measurement and procedure. However, in most cases, a limited number of parameters can afford a reasonable description of the detector characteristics under a wide variety of operating conditions. The only detectors considered here are those *whose output consists of an electrical signal that is proportional to the radiant signal power.* The parameters to be considered are the detector signal, detector noise, radiation signal power, detector bias, detector temperature, detector physical and electrical properties, and the background conditions under which the detector is operated. (See references 1 and 2 for discussions of these parameters.)

550-896 O - 74 -- 4

Based on these measurements, the following figures of performance can be calculated that enable a reasonable comparison between detectors:

- Noise equivalent input (H_N)—the minimum radiant flux density necessary to give a signal-to-noise ratio (SNR) of 1 for unit bandwidth.
- Noise equivalent power ($P_N = H_N A_D$)—the minimum radiant flux necessary to give an SNR of 1 for unit bandwidth, where A_D is the effective detector area.
- D-Star ($D^* = A^{1/2} P_N^{-1}$)—the SNR per unit incident flux for a detector assuming that signal and noise power are each direct functions of area. Thus, given this condition, D-Star describes a general type rather than one having a particular area.

D-Star is a very popular figure of performance, since it can be used to describe most semiconductor detectors. It must be used with caution, however, as all detectors *cannot* be described satisfactorily in this manner. Also, it should be noted that possible desired and necessary tradeoffs can be hidden when there is a noncritical dependence on D-Star or another comparable figure of performance. For example, Figure 1 shows the noise power spectrum of an indium antimonide (InSb) photoconductor with bias current as a parameter. In Figure 1a, the noise is monotonically increasing with bias current. However, the responsivity is such that the optimum detectivity occurs with a bias of 125 microamperes (μA), as shown in Figure 1b. In fact, the detectivity at 250 μA is degraded by only a small amount from the so-called optimum value, while the requirement for the

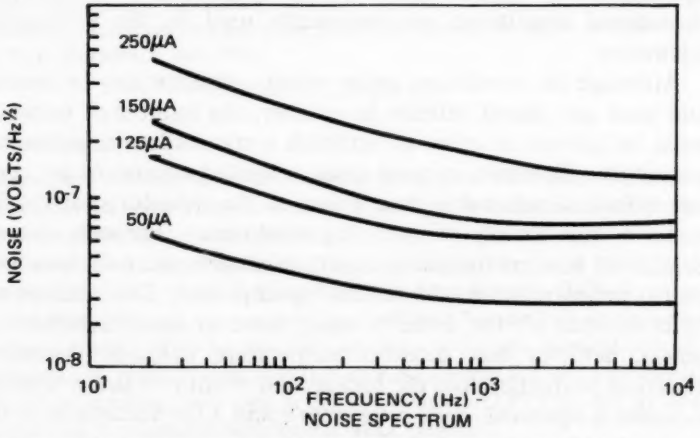

Figure 1a – Noise spectra for InSb photoconductor at several bias currents.

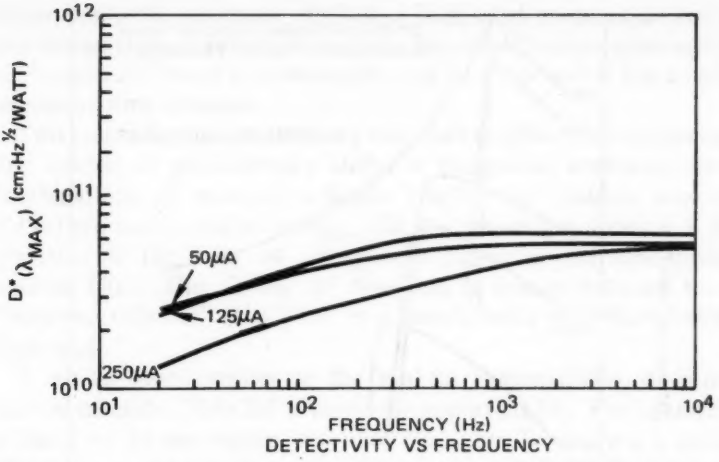

Figure 1b – D at the spectral wavelength at which responsibility is a maximum for bias currents. D* for 250 μA is not significantly less than that for 125 μA.*

noise figure for the necessary preamplifier can be relaxed by a factor of three or more. This is certainly a matter of significance to a design engineer.

Intrinsic and Alloyed Detectors

Two recent developments pertinent to IR technology can be described by comparing the detectivities of two classes of photodetectors. These are detectors that can be operated in conjunction with thermoelectric coolers (having a practical lower limit of approximately 200K operating temperature) and alloyed detectors.

The detectivities for five intrinsic photodetectors operated at 200K, as well as the theoretical limits for detectors exposed to a photon flux from a 300K background, are shown in Figure 2.

Lead sulphide (PbS) increases in D* about an order of magnitude upon cooling to 200K and approaches the theoretical limit. Unfortunately for some applications, the responsive time constant also increases by at least an order of magnitude. The temperature of 200K thus appears to be optimum for maximizing the D* of PbS. However, some high-performance cooled PbS detectors have exhibited reduced D* values when the detectors were exposed to relatively low levels of visible and ultraviolet radiation.

Lead selenide (PbSe) detectors also increase about an order of magnitude in D* when cooled to 200K. This temperature also

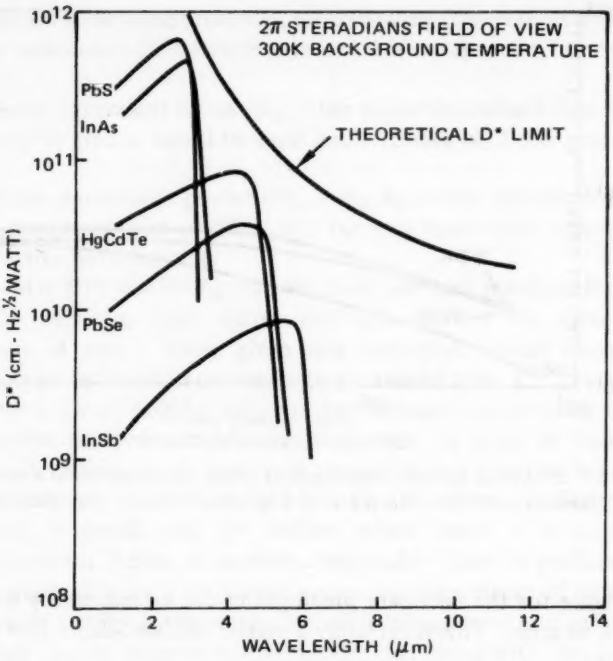

Figure 2 – Representative spectral D curves for several photodetectors operating at 200K. The theoretical curve gives the limiting value for D* with a 300K background.*

appears optimum for PbSe, and the specific detectivity approaches the theoretical limit. PbSe does not operate well over long periods of time in a hard vacuum, and this peculiarity has presented some problems when PbSe is operated cooled. However, a recent change in dewar design has largely solved this problem. Recent efforts for both PbS and PbSe have seen the development of cooled arrays using cold aperture stops, cold spectral filters, and thermoelectric coolers.

Indium arsenide (InAs) increases in specific detectivity about an order of magnitude when cooled to 200K. The responsive time constant of this detector material is in the range of 1 microsecond. Since the temperature range of 200K is suitable for the operation of InAs, this material can provide fast, sensitive, and reliable detectors in the 1 to 3 micrometer (μm) spectral region.

Although the specific detectivity of indium antimonide (InSb) increases from one to two orders of magnitude when cooled to 200K, this temperature range is not low enough to achieve maximum D*

values for InSb detectors. InSb has been used to some extent at this temperature, however, since it can provide D* values approaching 10^{10} cm-Hz$^{1/2}$/watt at wavelengths out to 6 μm and it has a short responsive time constant.

Two recent families of photodetector materials have been developed that consist of pseudobinary alloys of compound semiconductors. Combinations of mercury telluride (HgTe) and cadium telluride (CdTe) are now available as $Hg_{1-x}Cd_xTe$, where x is about 0.2, for operation in the 8 to 14 μm spectral region of the atmospheric window (3). This family of detectors is usually referred to as "merc-cad telluride" (HgCdTe), as a generic term with the subscript suppressed.

A similar story applies to the lead-tin chalcogenides, of which lead-tin-telluride (PbSnTe) is currently important (4). For operation in the 8 to 14 μm region, the alloy $Pb_{1-x}Sn_xTe$ where x is about 0.2 has been used as a photodiode. Curves for a PbSnTe photovoltaic detector operated at 77K and a HgCdTe photoconductive detector operated at two different temperatures but designed for 8 to 14 μm are shown in Figure 3. Reference 5 gives information on comparing

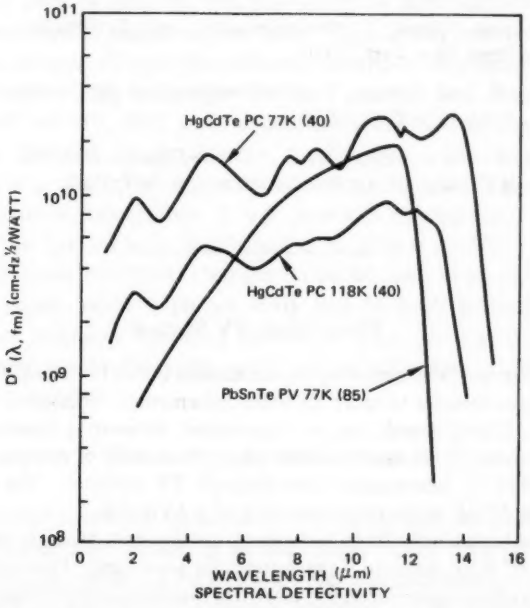

Figure 3 – Spectral D for a HgCdTe photoconductor and a PbSnTe photovoltaic detector shown at the indicated operating temperatures. The field of view (in degrees) is given in parenthesis.*

other detectors, in additions to further details and definitions of terms used in this paper.

Current Programs

A current program being conducted at NELC is directed at establishing definitive measurement techniques for characterizing detectors under extremely reduced photon flux conditions. This is very important because of the background-limited nature of most current and developing IR photodetectors. Another effort is aimed at measuring performance under certain radiation fluxes that alter the detector characteristics either temporarily or permanently.

The author wishes to acknowledge the assistance of his NELC colleagues, particularly W. L. Eisenman and J. D. Merriam.

References

1. Holter, M. et al, *Fundamentals of Infrared Technology,* MacMillan, New York, 1962

2. Krause, P. W., McGlaucklin, L. D., and McQuiskin, R. B., *Elements of Infrared Technology,* Wiley, New York, 1962

3. Long, D. and Schmit, J., *Semiconductors and Semimetals,* v. 5, ch. 5. Academic Press, New York, 1970

4. Melngailis, E. and Harmon, T., *Semiconductors & Semimetals,* v. 5, ch. 4. Academic Press, New York, 1970

5. Potter, R. F. and Eisenman, W. L., "Infrared Photodetectors: A Review of Operational Detectors," *Applied Optics,* v. 1, p. 567, 1962

Fiber-Optic TV System

A closed-circuit TV system recently installed in USS KITTY HAWK (CVA 63) uses fiber-optic bundles to carry the video information. Because of the low-loss cables (70 dB/km), signals can be transmitted between a transmitter and a receiver separated by as much as 1000 feet. The quality of reception compares well with that of conventional closed-circuit TV systems. The system was developed by NELC under the sponsorship of NAVELEX.

NELC has been conducting a technology development program leading to the application of fiber optics to Navy systems for some time. Fiber-optic technology provides advantages of security, electrical isolation between transmitting and receiving terminals, immunity to electromagnetic interference, and space and

(Continued on page 36)

Bioelectronics Research at NELC

C. T. White
Human Factors Technology Division
Naval Electronics Laboratory Center

NELC's Bioelectronics Research Group was established in 1957 to study the various bioelectric phenomena, develop improved techniques for dealing with them, and apply the findings of such work to general human factors problems. Early work in this area dealt with the problem of establishing the physiological cost of performing certain kinds of tasks, both physical and mental. Detailed studies were made on the learning of motor skills and the changes that occurred in the various muscle groups that were involved. Techniques were devised for integrating the electrical activity of the muscles so that meaningful quantitative work could be performed. Finally, a number of extensive studies were conducted and published on the effects of fatigue and motivation on performance and the electrical activity of the muscles.

Another area of interest was the study of how subjects use their eyes in performing visual search tasks. This study involved developing the technique of two-dimensional electro-oculography (EOG) to a usable level. This technique is based on the fact that the eye is like a small battery, that is, it is positively charged at the front and negatively charged at the back. As the eye moves in its socket, corresponding electrical changes occur in the dc field around it. NELC scientists found that it was possible to represent the movements of the eye on a dc oscilloscope or strip-recorder. It was also found that these electrical changes could be used as an effective control mechanism, since a person only has to look toward an object to bring an auxiliary tracking system to bear on that object. This characteristic could be very useful in developing certain kinds of prosthetic devices.

The Average Evoked Response

The development of practical techniques for recording minute electrical transients occurring in the brain when there is an abrupt stimulus change started a new era in the neurosciences, as well as in the Center's bioelectronics research program. The basic problem in trying to record such transient effects was the signal-to-noise ratio, since the transients are just a small fraction of the amplitude of the

ongoing electrical activity of the brain. However, since the transient effects are timelocked to the stimulus-change and the brainwaves are not, a number of such responses can be summated to obtain a record of changes in the electrical activity occurring at the surface of the scalp that is related in some way to the stimulus-change that produced those changes. Although this technique can be used to study any of the major sense modalities, NELC researchers decided to concentrate on vision. Therefore, a large number of parametric studies were carried out to gain familiarity with the newly-developed technique. Some of these studies are described in the monograph of White and Eason (1).

The Center's studies of visual pattern-evoked responses have proved to be particularly valuable. Figure 1 shows the results of one early study on this topic. A subject's responses to four different patterns–checkerboard, horizontal grating, concentric circles, and radial lines–are shown. Each tracing represents the summation of 100 responses from an electrode placed on the scalp over the visual cortex. Since all four patterns had the same average intensity, color, and other such characteristics, the marked differences shown in the record clearly illustrate that different visual patterns produce very different evoked waveforms. Since the checkerboard pattern produced the strongest response, it was used intensively in succeeding studies at NELC. At this point, it should be pointed out that the examples being given are representative of work being done at a number of laboratories throughout the world during this period. A complete review of work being done in the area of evoked potentials up to 1970-71 can be found in the book by Regan (2).

Further studies using the checkerboard pattern have shown that there is an optimal size pattern that can be used to produce the pattern-related response in the normal adult (3). It has also been found that the quality of the retinal image is a very important factor in terms of the evoked response. Figure 2 illustrates that a blurred image produces a very different response than a clearly focussed image (4).

Applications

Extensive studies conducted by the U. S. Army (5) and by the College of Optometry of the State University of New York (6) proved that NELC's evoked response technique was a valuable diagnostic tool. These studies not only corroborated the Center's earlier work, but showed how the technique could be used in a clinical setting in relation to many diseases of the eye. Programs using the technique

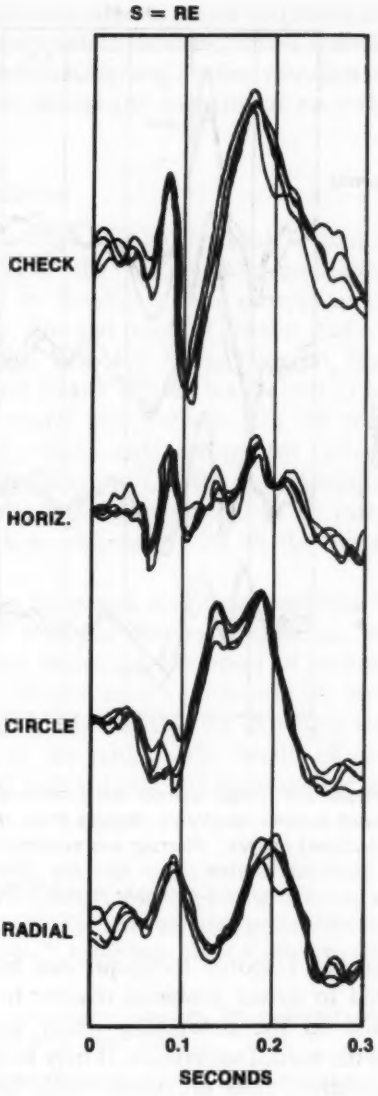

Figure 1 – A subject is a visual pattern-evoked responses to four different patterns have been recorded. Each tracing is the summation of 100 responses.

are now proceeding in schools of ophthalmology and optometry in many parts of the world.

The evoked response technique is especially well suited for dealing with individuals who cannot or will not respond adequately in standard testing situations. Perhaps the most important such group would be that of very young children. It has been demonstrated that the

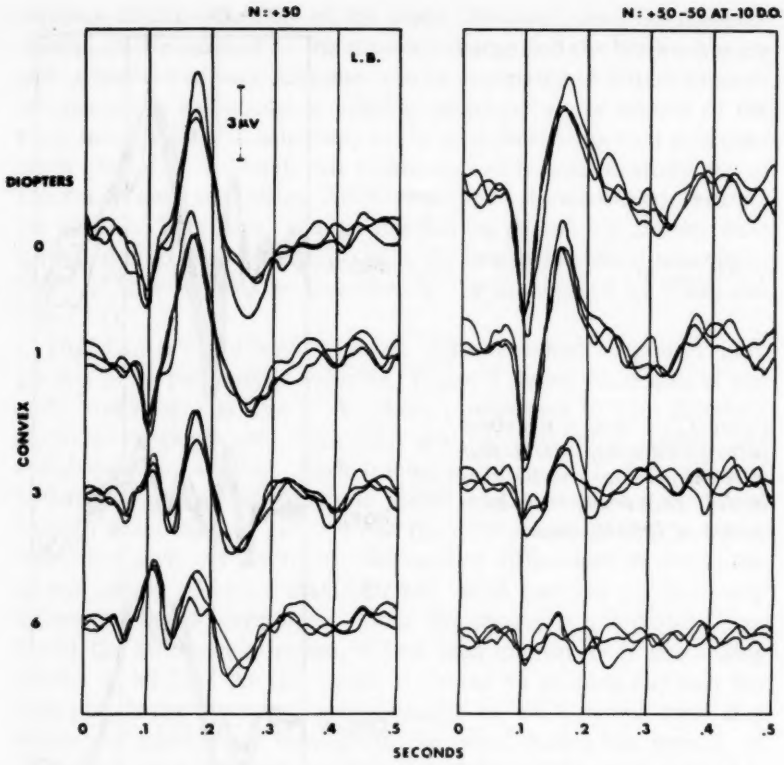

Figure 2 – Image quality has a marked effect on evoked responses. The left-hand column illustrates changes from sharp focus (top) to completely blurred (bottom) images. Blurring was accomplished by lenses of varying strength. The right-hand column shows how the effect can be increased by subtracting the response to pattern-free light flashes from the pattern responses.

evoked response technique can be used with children about 1 year old to detect problems relating to refractive errors and astigmatism and to the potentially much more dangerous amblyopia (6, 7). With special techniques, it may be possible to deal with even younger children, thus providing much needed diagnostic help during the most formative period of life.

The techniques evolved at NELC for the study of human adult and infant sensory responses can also be used for almost any other type of subject, including sea mammals (8). If relatively simple, noninvasive techniques could be made available for evaluating the sensory capacities of such animals, their already proven value in such tasks

as aiding man underwater and retrieving objects would be greatly increased. Preliminary screening could detect those individual animals incapable of certain levels of discrimination, and routine retesting of chosen animals should detect any changes in capacity at an early stage.

Conclusion

The two major long-range goals of NELC's bioelectronics research program are to better understand the information processing characteristics of the brain and to develop a new generation of neurological diagnostic techniques. The end result of present studies, both in-house and in collaboration with the Naval Hospital, San Diego and the San Diego Children's Health Center, is expected to be a set of very sensitive tests of neural effectiveness. In the very young, such tests would detect problems early enough for various ameliorative procedures to be undertaken, and, in the case of adults, detect the effects of adverse environmental conditions at an early stage. The Center's current work is concerned with all the major senses.

In working with the developing brain and with those individuals having known sensory deficits, it is hoped that techniques can be found for detecting subtle changes indicating the onset of various kinds of deterioration. The value of such tests is obvious in the case of young children, and should be equally valuable for detecting the onset of functional degradation in the adult. The results of the current work being done at NELC indicate that the development of such procedures is quite feasible.

References

1. White, C. T. and Eason, R. G., "Evoked Cortical Potentials in Relation to Certain Aspects of Visual Perception," *Psychology Monographs,* v. 80, Whole No. 632, 1966

2. Regan, D., *Evoked Potentials in Psychology, Sensory Physiology, and Clinical Medicine,* John Wiley and Sons, New York, 1972

3. White, C. T., "Average Evoked Potentials: Methods, Results, and Evaluations," *NASA SP-191* (Eds: E. Donchin and D. B. Lindsley), p. 118-124, 1969

4. Harter, M. R. and White, C. T., "Effects of Contour Sharpness and Check-size on Visual Evoked Cortical Potentials," *Vision Res.,* v. 8, p. 701-711, 1968

5. Duffy, F. H. and Rengstorff, R. H., "Ametropia Measurements from the Visual Evoked Response," *Amer. Journal Optom. and Arch. Amer. Acad. Optom.,* v. 48, p. 717-728, 1971

6. Ludlam, W. M. and Meyers, R. R., "The Use of Visual Evoked Responses in Objective Refraction," *Trans. N. Y. Acad. Sci.*, v. 34, p. 155-170, 1972

7. Lombroso, C. T., Duffy, F. H., and Robb, R. M., "Selective Suppression of Cerebral Evoked Potentials to Patterned Light in Amblyopia," *Electroencept. Clin. Neurophysiol.*, v. 27, p. 238-247, 1969

8. Naval Electronics Laboratory Center Technical Document 287, *Electroretinograms (ERGs) and Visually Evoked Responses (VERs) in the California Sea Lion (Zalophus Californianus)*, by J. I. Martin, C. T. White, R. W. Kataoka, and I. Stevens, 25 October 1973

(Continued from page 30)

weight saving. Frequency modulation minimizes the noise level in the wideband signal.

The combined advantages of fiber optic systems, particularly the space and weight reduction, point to possible future application in surface-effect craft where space and weight factors are critical.

The fiber-optic TV system operates as follows:

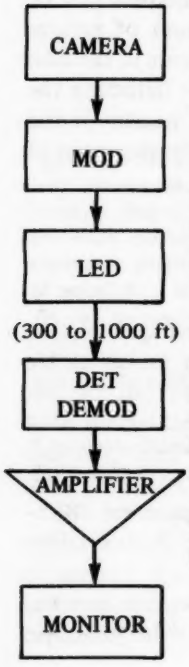

A 525-line camera provides a standard 1-volt, peak-to-peak, composite video signal.

The video signal modulates a voltage-controlled oscillator about its center frequency (44.3 MHz).

The modulated signal drives an infrared light-emitting diode (LED). (It should be noted that driving an LED by pulse frequency modulation, with attendant reduction in noise level, is a unique feature peculiar to the NELC system.)

The light signal passes through the fiber-optic cable to a detector-demodulator. The detector consists of an avalanche photodiode followed by two stages of wideband amplification and a limiter. The demodulator is a discrete phase-locked loop operating at the center frequency of the pulse frequency modulator (44.3 MHz).

The demodulated composite video signal (3-MHz bandwidth) is fed, via a buffer amplifier, into a closed-circuit monitor.

Modularized Digital Control

D. W. Doherty
Decision and Control Technology Division
Naval Electronics Laboratory

An increasing number of systems is being developed that require the use of a centralized or master digital computer to control one or more analog power drives. This is particularly true in the Navy, as evidenced by the trend toward using digital computers in gun and missile control and satellite tracking systems.

NELC has developed a digital controller that provides both digital interfacing between the master computer and the power drive and dynamic compensation of the power drive servo system. It is particularly applicable to the broad class of electrical and electrohydraulic power drives generally used in missile launchers, gun mounts, and tracking antennas. The controller, or "minicontroller" as it is called, has been developed using system modularity and eliminating as much redundant analog hardware as possible. The Center verified the universal nature of this controller from the results of a number of earlier studies. In these studies, digital controllers were developed for several different systems (e.g., the Tartar Mk 13 Guided Missile Launching System and the ASROC Mk 112 Launcher) using a general-purpose digital computer. In each case, there was a considerable degree of uniformity in both software programs used and system configuration.

When considering a hybrid application of this type, a primary concern should be that the master computer is not required to output position orders at an excessively high rate, thereby tying up valuable input/output time. This is particularly important if the computer is required to service more than one power drive at a time. It is usually desirable to limit the update or sample rate of position orders to about 32 samples per second. However, at this relatively low rate, some difficulty may be encountered in maintaining smooth system operation. For example, experience has shown that driving a conventional analog servo system at this rate (through a standard digital-to-synchro converter) would result in rough, unacceptable operation of the power drive and would probably cause premature component deterioration and overall poor response.

Other existing and proposed approaches to digital control typically require sophisticated digital-to-analog hardware. The interface usually involves some type of data extrapolation scheme and includes provision for digital-to-synchro (or resolver) conversion. In

this manner, the discrete, low sample-rate orders would be modified so they would be presented to the analog servo loop as a "quasi" continuous signal. These interfacing techniques, especially the associated analog hardware, are generally peculiar to a particular system.

In developing the minicontroller, NELC found that sample rates of 32 samples per second or less are readily acceptable if the servo control loop is closed digitally and the resulting digital error signal is operated on by suitable discrete control algorithms. The result is then applied to the power drive through an appropriate digital-to-analog converter. The minicontroller has been designed to provide digital compensation for as many as four independent axes—typically two two-axes systems or one three-axis system per sample period. State-of-the-art medium-scale-integration and large-scale-integration components have been used throughout the design.

System Description

Figure 1 is a functional block diagram of the minicontroller. Because position orders may be transmitted from the master computer in either serial or parallel form (depending on system requirements), a certain amount of signal conditioning is required. Similarly, the position feedback signal (shaft encoder, synchro-to-digital converter, etc.) usually requires some adjustment. Conditioning is generally limited to parallel-to-serial conversion and/or multiplexing and logic level shifting.

As is generally true with power drives, those applicable to this controller design are characterized by torque (acceleration) saturation. Thus, the control scheme used is based on a classical dual mode operation: A large signal or coarse control mode is used for large values of error to bring the plant to a nearly "synchronized" condition and then a linear control algorithm is used in the relatively narrow small signal region. Large signal control is accomplished by a switching curve that controls the plant deceleration at a predetermined rate and is based on a percentage of the maximum plant deceleration capability. This function is provided by the on-line solution of the fourth order polynomial in nested form:

$$V_c(n) = \left\{ [(c_4 E(n) + c_3)E(n) + c_2]E(n) + c_1 \right\} E(n) + c_0$$

where $V_c(n)$ is the solution of the polynomial, $E(n)$ is the present value of error, and c_0, c_1, c_2, c_3, and c_4 are constants. The small

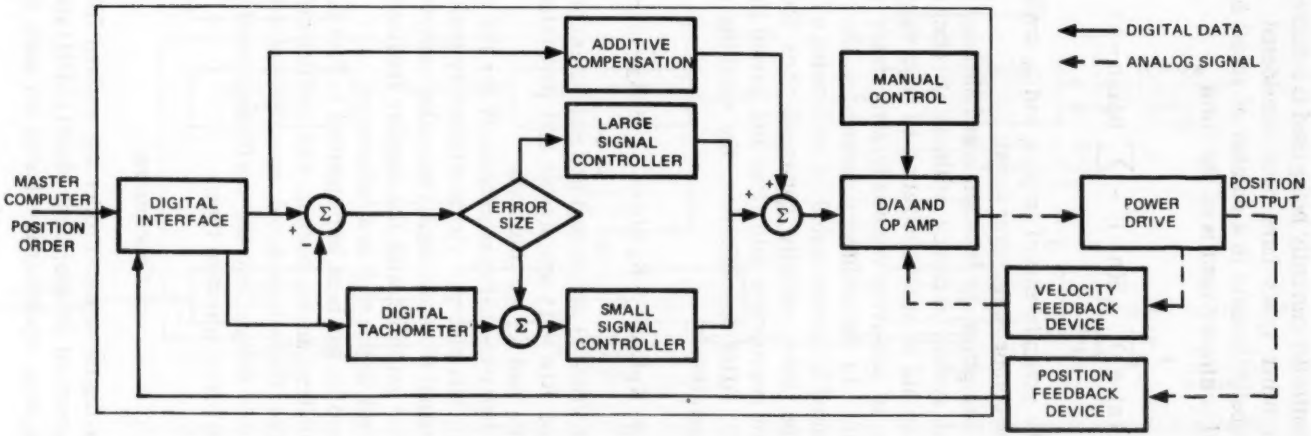

Figure 1 – Functional block diagram of the minicontroller.

signal (linear) controller currently being used is a discrete biquadratic lag. Although other types have been considered, this type has proven to be most successful in a number of actual hardware tests. The small signal controller used is of the form

$$\bar{E}(n) = \sum_{j=0}^{2} a_j E(n-j) - \sum_{k=1}^{2} b_k \bar{E}(n-k)$$

where E(n) is the present value of error, a_j and b_k are constants, and $\bar{E}(\cdot)$ denotes the compensated error signal.

The additive compensation function is included as a means of providing improved system accuracy without affecting stability. It serves as both an aid in synchronization to large signal commands, and as a means of achieving essentially zero steady state error to ramp-type inputs. In the additive compensator, the change rate of the input command is approximated by performing a first backward difference. The input velocity command thus formed is then multiplied by an appropriate gain term and passed through a first-order lag filter. After simplification, the resulting equation that describes this operation is

$$\bar{V}(n) = K_1 R(n) = K_1 R(n-1) = K_2 \bar{V}(n-1)$$

where $\bar{V}(n)$ and $\bar{V}(n-1)$ are present and past values of compensator output, R(n) and R(n – 1) are present and past values of position command, and K_1 and K_2 are constants.

A study of digital-to-analog requirements for the minicontroller indicates that 10 bits plus sign yields satisfactory performance. The analog output signal from the digital-to-analog converter is summed in the operational amplifier with the negative feedback provided by a velocity feedback device such as a tachometer.

The minicontroller has been implemented in four basic modules—processor, status/test, analog output, and coefficient/interface (see Figure 2). The first three listed are identical for all systems applicable to this design, but the coefficient/interface module is generally unique for each system type.

Conclusions

The Center's digital minicontroller has evolved from the breadboard to the Advanced Development Model (ADM) stage (Figure 3). The device has been operationally tested on such systems as the

Figure 2 – The minicontroller has been implemented in four basic modules. Although the coefficient/interface module is generally unique for each system type, the other three modules are identical for all systems applicable to this design.

Figure 3 – The Advanced Development Model (ADM) minicontroller has been tested on a number of operational systems, including a Mk 42 Mod 9 5"/54 gun located at the Naval Weapons Laboratory.

3"/50 caliber gun at NELC and the Mk 42 Mod 9, 5"/54 caliber gun at the Naval Weapons Laboratory, Dahlgren, Virginia, and is currently being adapted to the digital control of a 6" Ka-band antenna being developed at the Center.

Some of the advantages that the minicontroller has over other approaches to the problem are listed below:

- The response to large signal inputs approaches time optimal—exhibiting very little overshoot (< 0.1 degree).
- Its small size (less than 1/2 cubic foot) allows it to be mounted in the proximity of the particular power drive it controls.

- Off-the-shelf logic components have been used throughout, thus negating the requirement for high-risk, one-of-a-kind circuits.
- High tracking accuracies are achieved while maintaining smooth operation at a relatively low sample rate (20 to 32 samples per second).
- Several axes of rotation may be controlled, that is, two 2-axes systems, or one 2- or 3-axes system.
- Built-in test features eliminate the requirement for external devices such as "dummy directors" to perform routine operational maintenance and fault isolation.
- Since it is applicable to a large class of power drives, only minor modifications are required from one system to the next.

Antenna Study Completed

NELC has completed an hf antenna system design study for the Patrol Hydrofoil, Missile (PHM), a high-speed patrol craft being designed and built under Navy contract for use by NATO forces. The study was conducted because the short length (40 meters) of the PHM, coupled with the requirement for simultaneous operation of two 1 kW hf transmitting circuits, poses difficult antenna placement problems. The Navy's only automatic antenna coupler, the AN/URA-38, has serious interference problems when operated physically close to a second radiating source. Since there is not enough space on the PHM to install a broadband antenna with a multicoupler, alternate antenna designs and/or antenna coupler types must be used.

Work on the hf antenna subsystem design was performed at NELC's Ship Antenna Model Range using a 1/50-scale brass model of the PHM. This facility is used to measure radiation patterns and impedance of shipboard communication antennas. It was determined that the best antenna arrangement was a 10.7-meter, three-wire, bent-fan antenna strung from the mast aft and fed at deck level and a 5.33-meter whip antenna installed on the port side just aft of the pilot house. If needed, a second 5.33-meter whip could be mounted starboard for the backup receive circuit. The spacing between fan and whip at the nearest point is 9.75 meters. These two antennas will have the maximum isolation possible, will operate with reasonable efficiency, and will meet the near-field-level requirement for the PHM weapon system.

Optical Data Processing for Fleet Applications

R. P. Bocker, K. Bromley, and M. A. Monahan
Electro-optics Technology Division
Naval Electronics Laboratory Center

Because of the Navy's broad interest in signal processing, it is currently funding many programs to develop systems for performing transform and matrix operations. Potential areas of system application include Fourier spectral analysis of signals, vocoding and bandwidth compression of voice, and numerous applications to transversal filtering in radar and sonar signal processing. Most of the currently available systems for performing matrix transformations are all digital electronic systems that require either time-consuming sequential computations of each point in the matrix or large amounts of hardware to achieve some degree of parallelism in operation. Since most of these processors are "hard wired" to perform a particular sequential algorithm, they are capable of performing only one type of transformation. The electro-optical processor currently being developed by the Naval Electronics Laboratory Center is programmable to perform any one of a number of mathematical transformations at very high speed. The optical, fully-parallel nature of the device allows almost instantaneous computation of very large transformations in a unit that can be significantly smaller and less complex than existing systems.

The use of optics in signal processing introduces two important features. The first feature is an extremely fast multiplication rate—one analog value can be multiplied by another in the time required for light to pass through an optical transparency (about a picosecond). The second feature is the parallel processing capability—the two-dimensional nature of light propagation allows many one-dimensional operations to be performed simultaneously. Since the advent of the laser, much effort has been expended in applying *coherent* optical techniques to signal processing so that the separate control of amplitude and phase obtained could be utilized. However, in many applications, such efforts are being thwarted by (1) vibration sensitivity due to the interferometric nature of many techniques, and (2) the lack of a real-time input material sufficiently developed to a cost-effective, compact, off-the-shelf system. Fortunately, there are many worthwhile applications that do not require vibration insensitivity and real-time operation, and much promising research is being conducted to solve these problems in other applications.

NELC researchers chose to pursue a different tack—to investigate *incoherent* optical techniques. Such techniques have the features of fast multiplication rate and parallel operation but do not have the problems of vibration sensitivity and the lack of real-time input capability. Results of the Center's program to date have been very promising (1-4). Two early exploratory development models of NELC's electro-optical processor were designed to cross-correlate simultaneously a "live" input signal with a large reference library of stored signals. These systems were applied to the problems of automatic passive sonar classification and active sonar detection and localization (1, 2).

Figure 1 shows the most recent implementation of the Center's electro-optical processor. This system is capable of a large variety of linear transformations and linear filtering operations. The basic concept of the technique is described as follows: The electrical input signal modulates the radiance of a light emitting diode (LED) as a

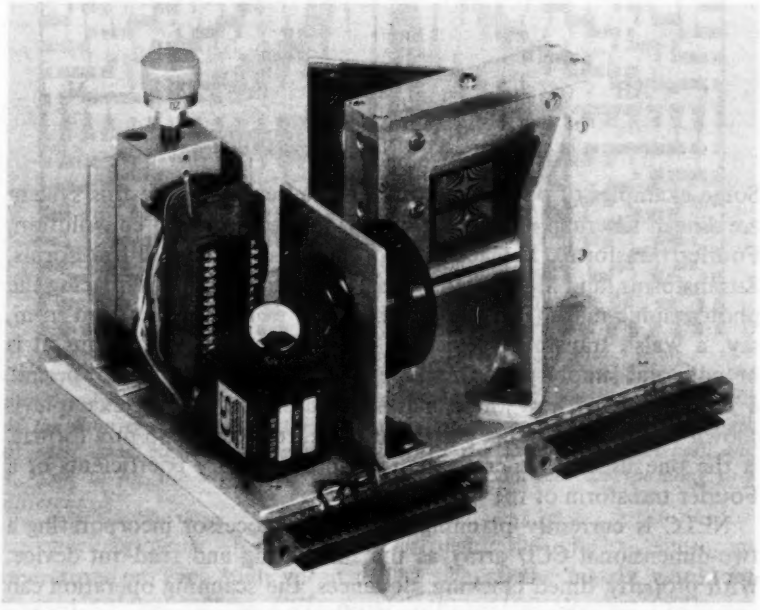

Figure 1 – Current implementation of NELC's programmable electro-optical processor. Components include the following: (1) light-emitting diode, (2) stationary mirror, (3) Fresnel condensing lens, (4) optical transparency, (5) stationery mirror, (6) imaging lens, (7) scanning mirror, and (8) linear charge-coupled device.

function of time. This LED is imaged by a Fresnel condensing lens into the entrance aperture of an imaging lens. In this light beam, immediately after the condensing lens, is placed a photographic transparency. This mask has the form of a linear array of horizontal channels with each channel having a different spatial vibration in intensity transmittance corresponding to some desired function. The imaging lens images this transparency, via a scanning mirror, onto a vertical row of integrating detectors—in the present embodiment, a linear charge-coupled device (CCD). The scanning mirror causes the image to repetitively translate horizontally, with constant velocity, across the face of the CCD array. The CCD integrates this intensity-modulated moving image during the mirror sweep. The resultant values are read out during the mirror's return.

In mathematical terms, the electrical input signal modulating the LED could be expressed as a column vector **B** of sampled data points, the mask as a matrix **A**, and the analog values serially read out of the CCD as a vector **C**. Then it can be shown that this device performs the vector-matrix multiply operation (4):

$$C = AB \quad \text{or} \quad c_m = \sum_{n=1}^{N} a_{mn} b_n, \quad m = 1, 2, 3, \ldots, M.$$

Some examples of operations that can be performed by this system are linear filtering, derivative operations, correlation, convolution, Fourier transforms, Laplace transforms, Walsh-Hadamard transforms, Z-transforms, and Mellin transforms. In fact, by simply replacing the photographic mask (i.e., the matrix A), it would be converted from, say, a Walsh transform device to a Z-transform device. Thus, it is broadly and simply programmable. Although space does not permit a description of how these masks are designed (4), an example is shown in Figure 2. This particular mask, reduced to 35 mm format, is the one used to generate the real and imaginary coefficients of a Fourier transform of the input data.

NELC is currently planning to build a processor incorporating a two-dimensional CCD array as the integrating and read-out device. With properly timed clocking sequences, the scanning operation can be performed entirely within the CCD chip, thereby eliminating the need for a scanning mirror. Such a system, composed of only an LED, a condensing lens, a replaceable mask, and a two-dimensional CCD array, will form an extremely compact, rugged, inexpensive system—with no moving parts—for performing vector-matrix

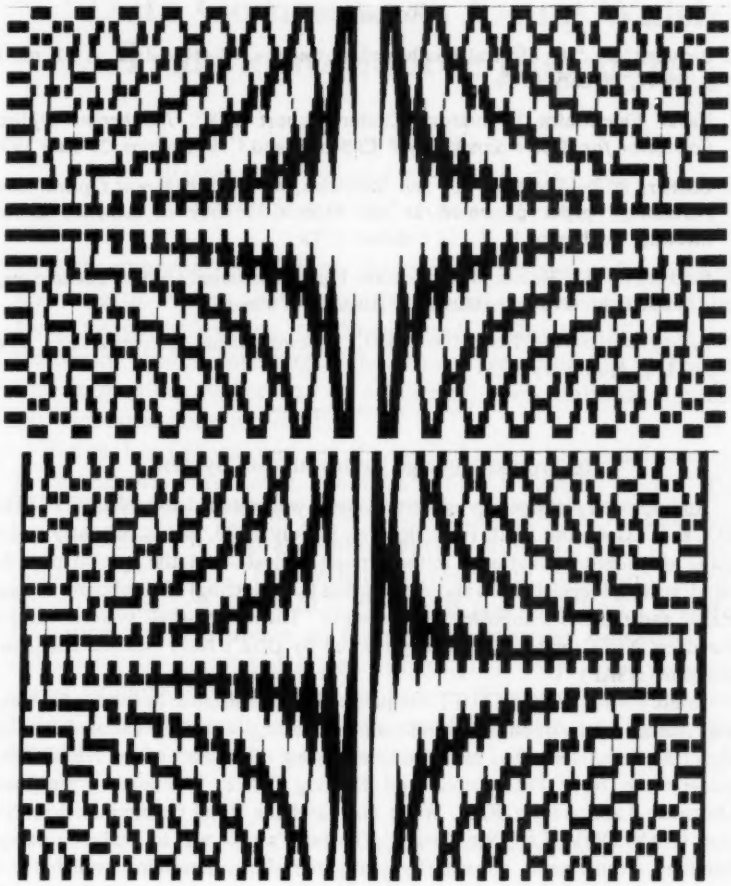

Figure 2 – When used in NELC's programmable electro-optical processor, the upper and lower halves of this mask produce the real and imaginary components of the Fourier transform coefficients of the input data. The horizontal length of each mask element is proportional to 1 + cos ω for the upper half, and 1 + sin ω for the lower half, with each horizontal line corresponding to a different ω.

operations at very high speed. The size of the matrix would be limited to that of the CCD array (100-by-100 element CCDs are off-the-shelf items today, and 1000-by-1000 element CCDs are envisioned within a few years). The fastest throughput rate would be limited to the readout rate of the CCDs (typically 10 MHz today, with peristaltic CCDs promising 1 GHz for the future (5)).

References

1. Bromley, K., "An Optical Incoherent Correlator," *Optica Acta*, v. 21, no. 1, p. 35-41, January 1974

2. Naval Electronics Laboratory Center Report 1887, *Incoherent Optical Correlator for Active Sonar*, by T. C. Strand and C. E. Persons, 27 July 1973

3. Bocker, R. P., Bromley, K., and Monahan, M. A., *Incoherent Optical Data Processing*, paper presented at the Optical Society of America annual meeting, Rochester, N. Y., 11 October 1973

4. Bocker, R. P., "Matrix Multiplication Using Incoherent Optical Techniques," *Applied Optics*, to be published in August 1974 issue

5. Anonymous, "And Now—the PCCD," *Electro-optical Systems Design*, v. 6, no. 1, p. 6, January 1974

Improved Message Reproduction System

An improved message reproduction system was installed aboard USS LITTLE ROCK (CLG 4), the Sixth Fleet flagship, in July 1973, and is currently undergoing shipboard evaluation. Initial reports indicate that the system provides rapid, accurate reproduction and distribution (i.e., slotting) of shipboard message traffic and reduces manpower requirements. The off-the-shelf system was procured by NELC under a project sponsored by DNL's Navy Science Assistance Program (NSAP).

In late FY 72, COMSIXTHFLT requested NSAP assistance in solving problems experienced in the duplication and manual handling of messages aboard the flagship. A project team was established consisting of members from NELC (team leader); the Navy Publications and Printing Office, Washington; the Naval Ordnance Laboratory (NOL), White Oak; and the Naval Communications Station (NAVCOMMSTA), San Diego. The team's task was to analyze message-handling requirements aboard flag-configured ships, determine availability of equipment to satisfy those requirements, and make recommendations to the Navy for procuring equipments based on competitive evaluation.

In July 1972, team members conducted a survey to determine the density of message traffic associated with flagships of all sizes. Assistance was provided by the Atlantic and Pacific type commanders. In September 1972, NELC and NPPS personnel visited the CVAs on Yankee Station in the Tonkin Gulf to verify message loading at its heaviest peaks. From the data gathered, a specification for shipboard message reproduction and collating equipment was generated and three qualified systems were tested at NAVCOMMSTA San Diego in March 1973. The SIXTHFLT Staff then selected the configuration, from the qualified vendor's system, to be installed on LITTLE ROCK. A microfiche system for message storage offered by one bidder was also tested and accepted for shipboard use.

(Continued on page 56)

Data Compression Using Walsh Transform Source Encoding

D. C. McCall
Decision and Control Technology Division
Naval Electronics Laboratory Center

Data compression of three to one can be attained in an image transmission system that transmits a coded version of a Walsh transform image rather than the image itself. This technique is called transform source encoding. The reason for using this technique is that it provides higher coding efficiency, computational simplicity, and increased noise immunity.

Figure 1 is a block diagram of a typical image transmission system. In the experimental work, the TRANSFORM SOURCE ENCODER, CHANNEL, and TRANSFORM SOURCE DECODER were simulated by software. A digital frame capture unit (DFCU) (Figure 2) acquired by NELC for evaluating candidate transform methods played the role of the IMAGE READER and DISPLAY. The Walsh transform, an expansion in terms of rectangular waveforms, was chosen for the simulated system because it is easy to implement, in terms of both software and hardware. Figure 3 shows an image before it was transmitted over the simulated system using the Walsh transform and after it was reconstructed. No loss of fidelity is apparent.

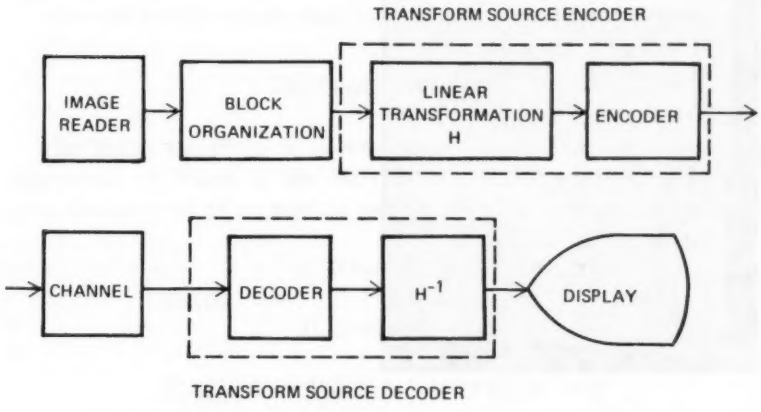

Figure 1 – Block diagram of image transmission system.

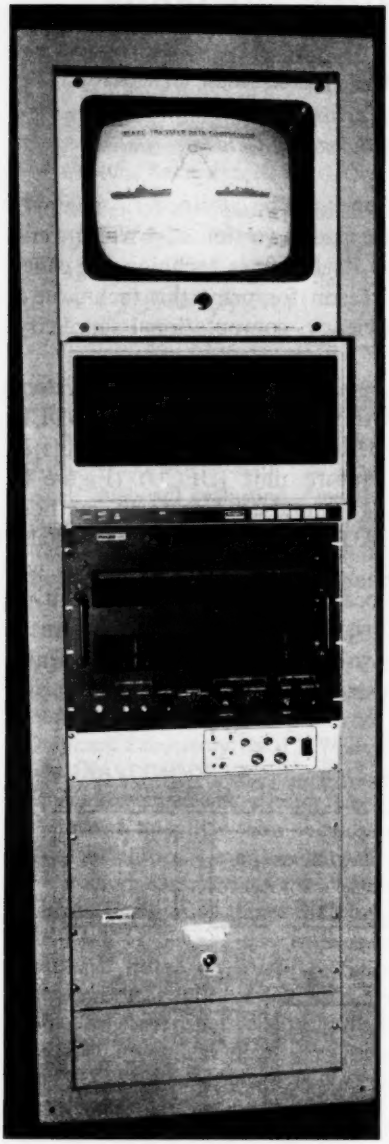

Figure 2 – The digital frame capture unit acquired by NELC is a combined video digitizer and single frame memory unit that converts conventional 525-line TV to a digital format for storage and subsequent computer processing. The DFCU is designed to interface with standard IBM-compatible digital tape transports for direct computer processing and provides for display, via TV monitors, of pre- and post-processed data.

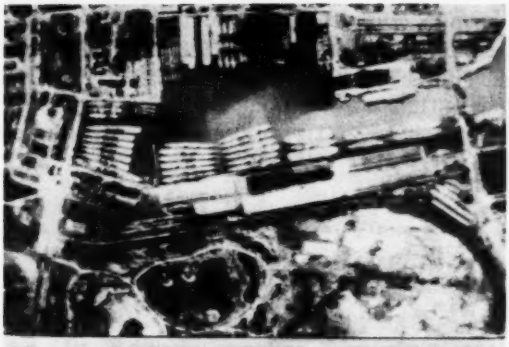

ORIGINAL 6 BITS/PIXEL

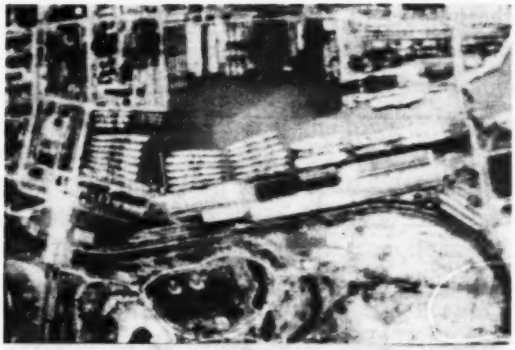

WALSH TRANSFORM 2 BITS/PIXEL

Figure 3 – A photograph before being transmitted over the simulated system using the Walsh transform (top) and after being reconstructed (bottom).

The Walsh Transform

The Walsh transform is derived using Walsh functions that were discovered by Walsh in the early 1920s (1). They can be defined over the interval from zero to one from the following relationship:

$$W_0(u) = \begin{cases} 1, & 0 \leqslant u \leqslant 1 \\ 0, & \text{otherwise} \end{cases}$$

$$W_{2j+p}(u) = W_j(u) + (-1)^{j+p} W_j(2u - 1)$$

$$p = 0, 1; j = 0, 1, \cdots .$$

Since these functions form a complete, orthonormal set over the interval zero to one, a function defined on that interval can be expanded in a Walsh series. Thus,

$$f(u) = \sum_{j=0} a_j W_j(u), \qquad 0 \leqslant u \leqslant 1$$

$$a_j = \int_0^1 f(u) W_j(u) du.$$

Figure 4 shows the first eight Walsh functions as determined by the relationship shown above. If "sequency" is defined as one-half the number of zero crossings per unit time, the set of coefficients

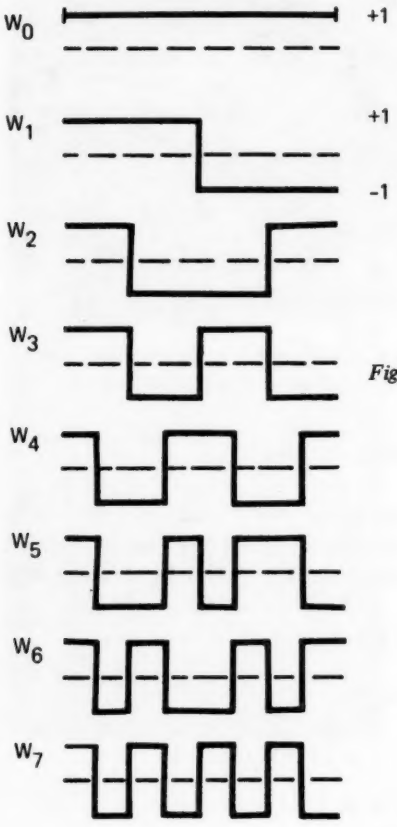

Figure 4 – The first eight Walsh functions.

$\{a_j\}$ in the Walsh series shown above represents the sequency spectrum of a function in the same sense that a series of Fourier coefficients represents the frequency spectrum.

The finite or discrete Walsh transform (DWT) (2) of the sampled version f(j) of the function f(t) is defined as

$$a(k) = \left(\frac{1}{\sqrt{N}}\right)\sum_{j=0}^{N-1} f(j)W_k(j), \qquad k = 0, 1, 2, \ldots, N-1,$$

where $W_k(j)$ is obtained by sampling $W_k(t)$ at the points $t = (j/N)^+$, and $(\ )^+$ indicates sampling from the right. This equation can be expressed in matrix form as

$$\underline{W} = (1/\sqrt{N})H\underline{f}$$

where $\underline{f}$ is the column vector of data, $\underline{W}$ is the column vector of Walsh coefficients and H is the transformation matrix, the rows of which are the sampled Walsh functions.

In the application of the DWT discussed below, N is restricted to be a power of 2, that is, $N = 2^n$. Figure 5 shows the 8 X 8 matrix H obtained by sampling the first eight Walsh functions as indicated above. Thus, DWT can be implemented by additions and subtractions of the data vector, plus a single multiplication.

Since H is a symmetric orthogonal matrix, the inverse transform is given by

$$\underline{f} = (1/\sqrt{N})H\underline{W}.$$

$$\begin{vmatrix} 1 & 1 & 1 & 1 & 1 & 1 & 1 & 1 \\ 1 & 1 & 1 & 1 & -1 & -1 & -1 & -1 \\ 1 & 1 & -1 & -1 & -1 & -1 & 1 & 1 \\ 1 & 1 & -1 & -1 & 1 & 1 & -1 & -1 \\ 1 & -1 & -1 & 1 & 1 & -1 & -1 & 1 \\ 1 & -1 & -1 & 1 & -1 & 1 & 1 & -1 \\ 1 & -1 & 1 & -1 & -1 & 1 & -1 & 1 \\ 1 & -1 & 1 & -1 & 1 & -1 & 1 & -1 \end{vmatrix}$$

H_8 – WALSH MATRIX OF ORDER 8

Figure 5 – The 8×8 matrix obtained by sampling the Walsh functions shown in Figure 4.

Thus, the forward and inverse transform have the same implementation. For $N = 2^n$ the DWT has a "fast" implementation similar to the fast Fourier transform. This fast implementation and the bivalued nature of H make the DWT extremely applicable in digital systems.

Encoding a Transformed Image

In the digital image transmission system diagrammed in Figure 1, the IMAGE READER digitizes the image, the BLOCK ORGANIZATION partitions the image into subblocks, and the TRANSFORM SOURCE ENCODER computes the Walsh transform and encodes the Walsh spectrum for transmission. At the receiver, the decoding and inverse transformation operations regenerate the image. The optimum source encoder would produce a vector $\underline{y}$ with components that are statistically independent. This would allow each component to be encoded independently and to be represented by only as many bits as necessary to retain adequate fidelity. Although the discrete Walsh transform is not optimum, it does produce a transform vector with components that are "nearly" independent. By treating these components as if they were independent, reasonable results can be produced.

To illustrate these concepts, consider a digitized image consisting of 480 rows and 640 columns, with each entry one of 64 possible gray levels (6 bits). (The Center's digital-frame capture unit can digitize images in this format.) The array is block-organized by partitioning it into 4 X 4 subarrays, as shown in Figure 6. Each subarray is processed independently, and a data vector $\underline{x}^j$ for the j^{th} subarray is formed by juxtaposing the rows of the j^{th} subarray, that is,

$$\underline{x}^j = (x_{11}, x_{12}, x_{13}, x_{14}, \ldots, x_{43}, x_{44})^T$$

where T denotes matrix transpose.
For convenience, the components are normalized by subtracting 32 from each component, and the DWT of $\underline{x}^j$ is computed. With $\underline{y}^j = (1/\sqrt{16})H\underline{x}^j$, the components of $\underline{y}^j$ are treated as if they were independent, and each is independently encoded.

The data reduction is accomplished in the encoding section shown in Figure 1 by using "tapered" quantization. In tapered quantization, fewer bits are allocated to components having less information. The

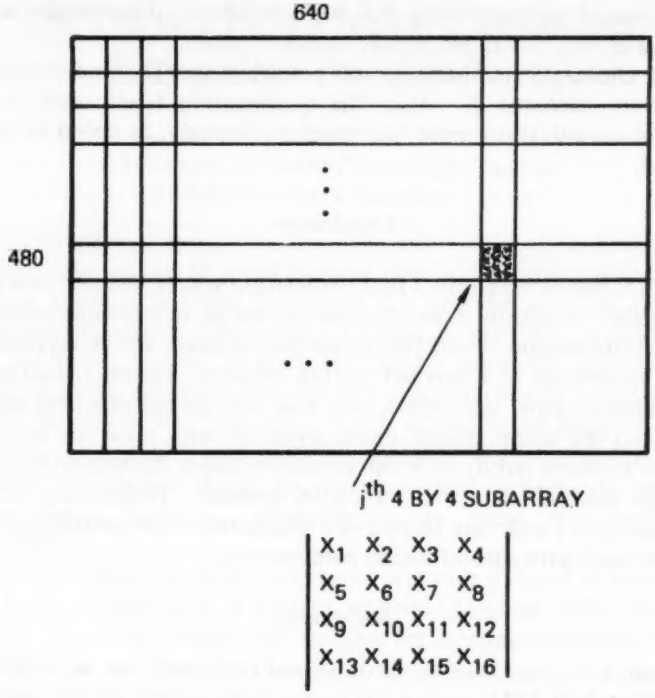

Figure 6 – A digitized image consisting of 480 rows and 640 columns is block-organized by partitioning it into 4 X 4 subarrays. Each subarray is processed independently.

bit distribution used in the system diagrammed in Figure 1 is shown below:

Component	Bits
y_0	6
$y_1 - y_2$	8 (4 ea)
$y_3 - y_6$	12 (3 ea)
$y_7 - y_9$	6 (2 ea)
$y_{10} - y_{15}$	0
	32

Since 96 bits are intially required to represent the spatial coefficients of each subarray and only 32 are required by using the system shown above, a 3 to 1 reduction in the number of bits used

to represent each subarray has been achieved. This results in an average of only 2 bits per picture element (pixel).

The choice of bit distribution is not arbitrary. This is discussed in detail in reference 3. Also, the quantization levels used in the tapered quantization must be chosen judiciously, as noted in reference 4.

Conclusion

NELC has demonstrated that a transform source encoder based on the Walsh transform is an effective means of data compression for image transmission. Using this technique, an image can be represented with an average of 2 bits per picture element. Hence, reduction in transmission time, bandwidth, and bulk storage requirements can be obtained by using digital image systems with such an encoder.

The bivalued nature of Walsh functions makes the implementation of this method attractive for digital systems. Preliminary studies indicate that a real-time version of a Walsh transform source encoder can be built with current digital components.

References

1. Walsh, J. L., "A Closed Set of Orthogonal Functions," *Am. Jour. of Math.* v. 45, p. 5-24, 1923
2. Andrews, H. C., *Computer Techniques in Image Processing,* Academic Press, New York, 1970
3. Purdue University School of Electrical Engineering Report TR-EE 70-2, *Linear Transformations for Encoding Two-dimensional Sources,* by A. Habibi and P. A. Wintz, March 1970
4. Max, J, "Quantizing for Minimum Distortion," *IRE Transactions on Information Theory,* v. IT-6, p. 7-12, March 1960

(Continued from page 48)

The message reproduction and storage systems were installed on LITTLE ROCK prior to the ship's departure for the Mediterranean area. During the period 1-30 September, the system processed over 1600 messages per day (over 2 million pages). Reliability and accuracy were high, and manpower requirements were reduced. A second system, similar in operation to that on LITTLE ROCK, has been installed for evaluation on USS KITTY HAWK (CVA 63).

A New High Order Computer Language for the Navy

W. E. Loper
Advanced Software Technology Division
Naval Electronics Laboratory Center

An extensible programming language called CS-4, which is designed to meet the needs of naval tactical data, command control, and avionic systems is being developed. It will be used on the All Applications Digital Computer (AADC), a modular configurable and extensible system of high level digital computer components, which is being developed by the Naval Air Systems Command for use in the 1978-1990 time frame (1-7). CS-4 is being designed with the hope that it will eventually become the successor to Compiler Monitor System-II (CMS-2), the Navy's current tactical data systems programming language. Development is being sponsored by NAVAIR.

CS-4 is a block- or module-oriented language defined in terms of, and as an extension to, a nucleus or kernel language called METAPLEX. All of the definitional facilities for creating extension sets in METAPLEX are available in CS-4. Since the design emphasizes building blocks rather than elaborate user-oriented features, new capabilities of expression and operation can be added in an easy, compatible manner. Thus, language power can be extended without opening the compiler or the CS-4 language to redesign.

A major design goal of CS-4 is the achievement of a high degree of machine independence without sacrificing the language's capability to exploit the potential of the architecture of a given computer hardware system or module. This has been accomplished by providing definitional facilities for high-level language constructs. Although these constructs are expressed in high-level, machine-independent terms, they may nevertheless be implemented on and fully exploit available hardware facilities. The expression and use of a programming feature is thus separated from the implementation of that feature. By segregating machine-oriented statements, they can be directly recoded, with minimum effort, for use on a different hardware system. This characteristic significantly reduces the cost of transporting programs from one hardware environment to another.

Although many of the definitional facilities would be available to all users, others would serve a more restricted purpose. The use of

these restricted facilities is expected to be limited to a system programming group of language maintainers, which would be the only group with both the capability and the administrative authority to make significant use of such capabilities. The language system implementation itself would contain a mechanism to enforce this control. The restricted facilities could be used by the system programming group for such tasks as defining problem-oriented languages. These languages, unlike procedure-oriented, imperative, and ordered languages (e.g., CS-4, JOVIAL, CMS-2, and FORTRAN), are preferably descriptive and essentially unordered, that is, the order of expression is not necessarily related to the order of correct execution. Examples of problem-oriented languages are those to be used for data base query, operations order planning, tactical exercise simulation and evaluation, and man-machine interface. Already a signal processing language and a device-independent display formatting language based on the work of Newman (8) are being developed as extensions of CS-4.

A very real goal of the CS-4 development is to protect the Navy's investment in existing CMS-2 programs. It should be noted that the characteristics of CMS-2 that most interfere with the transportability and reusability of programs are significantly responsible for the CS-4 development. However, certain portions of the CMS-2 software literature are valid and current. To ensure that these portions will remain usable, a conversion aid in the form of a translator program is planned for their recapture.

The CMS-2 language allows unregulated use of assembly language statements mixed with source text and offers data structure declaration forms in which machine characteristics such as word length and bit position form the basis for the definitions. While alternate, machine-independent forms are also provided, the alternatives are not strongly distinguished and may be freely mixed. A goal of the CS-4 language, on the other hand, is to confine machine dependencies to small, visibly bounded domains and to provide features that relieve the necessity of resorting to machine-dependent coding. Thus, a machine-dependent data structure definitional capability that is clearly identified for use in defining new data modes (or types) that do not map well onto the language's predefined primitives is available in CS-4. New operators can be defined on these new data structures and old operators extended to them. Recursive composition of data modes in terms of both the new and predefined primitives is supported, as well as operator definition and extension for the newly composed modes. A part of this capability is the

Generic Function. By this means, the compiler can be informed of, and can therefore apply, mode checking rules and conversions that are user-defined. Operators may be defined as commutative or noncommutative or left or right associative. They may be given precedence in terms of other operators or all may have the same precedences.

Facilities found in CMS-2 for overlaying data of different modes (data types) are absent and specifically prohibited from CS-4. Instead, there are free-space management techniques that can be applied by the compiler at compile-time. This means that run-time inefficiencies can be avoided, which must be the case in real-time, time-critical applications. CS-4 procedures may be specified to be open (in-line), closed (out-of-line), or heuristic (compiler decides).

All six characteristics of macros (patterns for open subroutines) required by McIlroy (9) are present in CS-4. In addition, the full power of the language is made available to users both at compilation and execution time. Two forms of compile-time function invocations are supported. One occurs at the lexical analysis level when the name of a substitution macro or lexicon (which is a user-defined string function of a string argument list) is scanned in the source test. The other occurs during the several walks of the tree formed by the parser and the semantics analyzer. The latter is triggered by the walking of a treenode corresponding to invocation of a function declared with the compile-time attribute. These compile-time capabilities are useful for implementing source-text substitution, code generation, and many other functions.

Application packages can be developed containing definitions that can be accessed in an independently compilable module. Accessed modules reveal to their interface only that part of their internal construction that is necessary for their use (e.g., mode definitions when variables of the declared mode must be declared by users of the module, procedure names when these must be callable, etc.). The remainder, which is not specifically made externally accessible, is invisible externally. This limits the degree to which a module can or must be used in terms of its internal construction and gives much more meaning to the concept of modular programming.

Mode checking is performed rigorously, both in binding together independently compiled modules and in compiling a module. Data descriptive of the interface of a module that is gathered during that module's compilation is preserved and reused automatically during compilation of accessing modules. Thus, there is no need to include potentially unreliable human expression of such information in the

source text of the accessing module. Top-down implementation is nonetheless possible by explicitly loading a module interface descriptor for a module that has not yet been compiled. Maintenance level and change data are recorded when the module is compiled. Binding will not occur unless the predicted and actual interfaces match.

CS-4 is a powerful programming language intended to support military applications through the exploitation of modern techniques of programming system development. Along with the language definition, an operating systems interface definition is being developed that will eliminate the need for rewriting programs when they are moved from one computer and its associated operating system to another.

References

1. Nissen, S. M. and Wallach, S. J., "The All Applications Digital Computer," *Proceedings of a Symposium on High-level-language Computer Architecture,* November 1973 (Available from the Association for Computing Machinery (ACM), P.O. Box 12105, Church Street Station, New York 10249 as SIGPLAN NOTICES, v. 8, no. 11. November 1973)

2. Naval Research Laboratory Report 7704, AN/UYK-17 *Signal Processing Element Architecture,* by W.R. Smith, J.T. Ihnat et al, 1974

3. Naval Air Systems Command Report, *All Applications Digital Computer Development Program Progress Report Number 11,* by R. S. Entner, 1 June 1973 (Previous program reports are titled *Advanced Avionics Digital Computer Development Program;* all 11 reports are available from National Technical Information Service, Springfield, VA 22151)

4. Miller, J. S., "A Programming Language Family for the Navy AADC," *Proceedings of ACM SIGPLAN-SIGOPS Interface Meeting on Programming Languages and Operating Systems,* held at Savannah, GA, April 1973, p. 115-116 (Also see p. 18-19 for Miller's discussion of synchronization techniques of the HAL language)

5. Loper, W. E., *CS-4 High Level Language and its Use in Real-time Systems,* paper presented at NATO/AGARD Avionics Panel Technical Meeting on Real-time Computer-based Systems, Athens, Greece, 27-31 May 1974 (proceedings to be released by AGARD)

6. Intermetrics, Inc., *CS-4 Language Reference Manual,* by J. S. Miller, C. M. Mikkelsen et al (available from NTIS)

7. Intermetrics, Inc., *A CS-4 Primer, Volume I, Basic Features,* by R. Fourer (available from NTIS)

8. Newman, W. M., "Display Procedures," *Communications of the ACM,* v. 14, no. 10, October 1971

9. McIlroy, M. D., "Macro Instruction Extensions of Compiler Languages," *Communications of the ACM,* v. 3, p. 214-220, April 1960

QED: Direct Functional Implementation of Electronic Systems

N. L. Tinklepaugh and D. C. Eddington
Advanced Digital Systems Architectural Division
Naval Electronics Laboratory Center

Very early in the evolution of the digital computer, system designers realized that the tedious task of programming registers, accumulators, and memory transfers to implement complex system functions created a severe burden on programmers and increased system development costs. As a result, high-level programming languages, such as APL, Algol and PL/1, were developed. These languages allow designers of computer-based systems to implement their functions without becoming buried in the details of gate interconnections, assembly level microinstructions, and complex bookkeeping required to perform sophisticated functions with simple "shift-and-add" central processing units. Today, a system designer can specify a system at the highest level functions, and then reduce these functions to the machine instruction level by using compilers, assemblers, and program coding. However, this practice results in a system that uses much more program memory and execution time than that which is actually required. When system speed is critical, operations must be hand coded in assembly language to bypass the normal inefficiency of compilers. As a result, the cost of software development and support can be as much as ten times the hardware cost.

Recognizing this problem, computer manufacturers have added more and more special-function hardware to their central processors. It appears that the competitive computer manufacturers are in a race to see which one can add the most high-level hardware functions to reduce programming effort and operating times. Unfortunately, even though special hardware has been added, the basic CPU hardware has remained essentially sequential, that is, it performs only one operation at a time.

Quick and Easy Design (QED) is a new approach to digital system architecture that is directed at simplifying design through the use of high level hardware modules. The QED project is part of the Naval Electronics Laboratory Center's Program 2175, which is directed at demonstrating at least a 2 to 1 improvement in life-cycle costs of

Navy electronic systems by Fiscal Year 1975. QED is dedicated to the design and development of a family of standardized modules that can be used in Navy digital systems.

By equating high-level functions to hardware modules, systems may be built from hardware building blocks and architectures suitable to the system's needs. These modules, by virture of greater internal complexity, can reduce the number of parts in a given electronic equipment. With fewer parts, there will be fewer interconnections, and thus fewer details for a designer to cope with. A simpler design results that can significantly reduce software and memory requirements. Control is maintained by simple supervision of data transfers to the processing function blocks. The speed and program bookkeeping limitations of sequential CPUs can be overcome by assembling processor hardware in which several functions can be performed simultaneously by parallel modules when needed. The control required for parallel operation is relatively simple. Control and processing hardware in such a system can be expanded in modular increments to accommodate system changes and upgrading of accuracy as performance requirements change after the system is in the field.

The QED Standardization Concept

Present trends in standardization of computers for military systems lean toward replacing a diversity of large commercial processors with a standard minicomputer. Weight, size, cost, and throughput requirements of military systems dictate that hardware be tailored to specific system requirements to reduce system executive, monitoring, and control software, and to eliminate unnecessary general-purpose hardware. QED is seeking modular standardization at a level that is low enough to allow large-scale-integration (LSI) implementation and wide application to many kinds of systems, but high enough to permit easy design at the functional level rather than at the medium-scale-integration (MSI) component level. Standardization is aimed at reducing system design and development time and costs by providing available off-the-shelf modules that can be readily interconnected and controlled. Likewise, total system life-cycle and logistics costs can be reduced by minimizing the total module population base to a set of standard modules. The QED approach is the implementation of a family of complete mathematical algorithms, control and input/output functions, and memory on a set of standard modules. The functions implemented are those of the APL programming language.

The APL Language

QED functions are derived from a high-level computer programming language called APL, which is based on K. E. Iverson's notation published in his book entitled "A Programming Language." This language identifies both computing and data processing procedures of functions from a problem-solving point of view rather than from an instruction set that is constrained by available computer technology. As a result, APL is a very concise language that allows problem solutions to be defined with a minimum of detail. The types of functions in APL are math functions–scalar, vector, and matrix–and data manipulation functions operating on character strings and arrays.

QED Module Function

A real-time processing system can be partitioned into four types of basic functions–mathematical/logical operations, memory, input/output interfacing, and control.

The mathematical/logical operations for the QED family were chosen from the functions of the APL programming language. The objective of the math function selection for the QED module set is to implement the primitive operators from APL as single module packages. These primitive operator modules can then be directly interconnected to form higher level math functions and array operations as defined by APL. The selection of math function groups for QED module partitioning was based on using available MSI devices and combining several functions into each module, with the objective of reducing the total module set.

Real-time processing requires memory any time that data or control instructions must be stored, either temporarily or permanently. QED modules have been defined to use off-the-shelf memory devices plus some internal control to achieve first-in first-out (FIFO), read-only memory (ROM), random-access memory (RAM), first-in last-out (FILO), and register file.

QED input/output interface modules provide signal conversion, impedance matching, interface control lines, and line driving/terminating necessary to convert incoming signals into digital formats for internal use and to reconvert digital system outputs to the signal formats of output devices. External interface modules have been defined for direct compatibility with standard interfaces such as MIL-STD-188 serial data, EIA RS-232 serial data, and the Navy

Tactical Data System. Interface conversion modules have been defined for analog-to-digital and digital-to-analog conversions. All data transfer is parallel, and all control and data lines are at transistor-transistor-logic levels. New interface modules can easily be defined as system requirements change or new peripheral devices are added. External interface characteristics can be changed modularly with minimal impact on internal operation of the system. This approach will result in a considerable reduction in the turn-around time (and expense) for reconfiguration or upgrading of a system.

The two categories of control functions are those required for overall system control and those for the control of complex higher level math functions (parallel and sequential control of composite math functions). Control functions at the system level include those of clock and timing generation, test and monitoring of internal and external status lines, program branching, and the transfer of system control under certain conditions such as a complete or partial system failure. Functions for control of complex math functions are those special functions required to tie several smaller primitive math modules together to form a special function, which then appears as a self-contained module to the overall system controller. For example, the normalizer interconnects several fixed-point modules into a larger, self-normalizing floating-point math function. A number of control functions have been identified for the current NELC program. They include timing sequence generator priority encoder/interrupt control, program decoder, bus switch, address generation and translation, normalizer, and counter modules. The control functions are tailored to control the math modules for easy implementation of vector and array operations specified in the APL language.

Other QED Features

Two of the most important features of this modularity program, particularly for shipboard installations where Mean-Time-to-Repair (MTTR) is highly critical and supplies are not readily available, are the on-line and off-line testing capabilities of the QED modules. The on-line test philosophy includes the capability of each module to be completely exercised by external system level test controllers, built-in test circuits on those modules that cannot be externally diagnosed, and provisions for dynamic system self-repair by fallback to spare modules. Off-line test philosophy provides for common hardware and pin assignments so that standard test jigs can be used to diagnose any QED module.

U.S. GOVERNMENT PRINTING OFFICE : 1974 O - 550-896

The physical characteristics of the QED modules allow them to be implemented in any 80-pin type package and in any component technology (TTL, metal-oxide-semiconductor, etc.). To provide rapid turnaround for development of the family of modules, an existing standard package was selected for initial implementation. This package is an expanded version of the Navy Standard Hardware Program 2A module. The chief advantage of this packaging is that systems can be developed from breadboard to engineering modules without changing system backplane wiring or repartitioning the circuit.

NAVAL RESEARCH REVIEWS publishes highlights of research conducted by Navy laboratories and contractors and describes important Naval experimental facilities. Manuscripts submitted for publication, correspondence concerning prospective articles, and changes of address, should be directed to Code 109, Office of Naval Research, Arlington, Va. 22217. Requests for subscriptions should be directed to the Superintendent of Documents, U.S. Government Printing Office, Washington, D.C., 20402. Subscription price: $4.50 per year in the U.S. and Canada; $5.65 per year, foreign; $0.45 per individual copy. The issuance of this periodical approved in accordance with Dept. of the Navy publications and printing regulations.

Editor: WILLIAM J. LESCURE

NAVSO P-510

Assistant Editor: CAROLYN J. SMITH

Associate Editors:

A. R. LAUFER, ONR PASADENA

A. R. DAWE, ONR CHICAGO

A. L. POWELL, ONR BOSTON

D. A. PATTERSON, NAVAL RESEARCH LABORATORY

IN THIS ISSUE

VOL. XXVII, NO. 5-6

Radio Propagation in a Marine Environment..... J. H. RICHTER AND H. V. HITNEY 2

RF Susceptibility of Microelectronic Components..... A. R. HART 12
D. W. MCQUITTY AND N. K. WAGNER

Equatorial Scintillation.....R. U. F. HOPKINS AND M. R. PAULSON 17

Performance Measurements of Infrared Photodetectors..... R. F. POTTER 25

Bioelectronics Research at NELC.....C. T. WHITE 31

Modularized Digital Control..... D. W. DOHERTY 37

Optical Data Processing for Fleet Applications..... R. P. BROCKER 44
K. BROMLEY AND M. A. MONAHAN

Data Compression Using Walsh Transform Source Encoding..... D. C. MCCALL 49

A New High Order Computer Language for the Navy.....W. E. LOPER 57

QED: Direct Functional Implementation of Electronic Systems..... N. L. TINKLEPAUGH 61
D. C. EDDINGTON

Cover Caption

Artist's concept showing several aspects of NELC's mission, which is to be the Navy's principal RDT&E Center for electronics technology and command control and communications and systems.

DEPARTMENT OF THE NAVY
OFFICE OF NAVAL RESEARCH
ARLINGTON, VA. 22217

OFFICIAL BUSINESS

PENALTY FOR PRIVATE USE, $300.

POSTAGE AND FEES PAID
DEPARTMENT OF THE NAVY
DoD-316

U.S.MAIL